



Université Mohamed Khider de Biskra
Science et technologie
Génie mécanique

MÉMOIRE DE MASTER

Domaine : Sciences et Techniques
Filière : Génie Mécanique
Spécialité : Mécanique énergétique

Réf. :

Présenté et soutenu par :
Mohamed Aymene BARKAT

Le : dimanche 6 septembre 2020

Study and construction of a Darrius type vertical axis wind turbine

Jury :

M.	Mounir DJELLAB	MCB	Université de Biskra	Président
M.	Foued CHABANE	MCA	Université de Biskra	Encadreur
M.	Salah GUERBAI	MCB	Université de Biskra	Examineur

Année universitaire : 2019 - 2020

DEDICATION

My parents:

My mother, who worked for my success, with her love,

**My father, who can help and find here the result of long years of
sacrifice and deprivation to help me move forward in life.**

**Thank you for the noble values, the education and the permanent
support that came from you.**

**My brothers, sisters and to the whole family who have been always
beside me to work hard and pursue my goals**

**To all who sacrificed their time for science and to all
those who use science for the good and prosperity of mankind.**

ACKNOWLEDGEMENTS

Above all, I thank Allah for giving me the courage and patience that have enabled me to accomplish this small and modest work.

Thank you to my supervisor, Dr Fouad CHAABEN, for consistent support, guidance and feedback, throughout this project and Special gratitude for his enormous support during the experimental setup.

Furthermore, I would like to thank the rest of the undergraduate research team for their collaborative effort during data collection.

I am grateful to all of those with whom I have had the pleasure to work during this and other related projects.

Finally, many thanks to all participants that took part in the study and enabled this research to be possible.

LIST OF SYMBOLS

Symbol	Explanation
A	Rotor Area
D	Overall Rotor Diameter
d	Blade Diameter
H	Rotor Height
V	Wind Velocity, m/s
N	Revolution per Minute
ω	Angular Velocity, rad/sec
ρ	Air Density, kg/m ³
λ	Tip Speed Ratio
C_p	Power Coefficient

LIST OF FIGURES

CHAPTER 1 : Wind energy

Figure 1.1: Electricity generation and power sector CO ₂ emissions in advanced economies, 1971-2019	1
Figure 1.2 : Total installations onshore.....	2
Figure 1.3: Various concepts for vertical axis turbines (Eldridge, 1980)	3
Figure 1.4: Savonius rotor.....	4
Figure 1.5: Different types of Darrieus rotor.....	5
Figure 1.6: Combined Savonius and Darrieus Rotor.....	5
Figure 1.7: Combined Savonius and Darrieus Rotor.....	5
Figure 1.8: Historic development of total installations.....	6
Figure 1.9 : Total Installed Capacity [MW].....	7
Figure 1.10: Onshore wind power generation in the Sustainable Development Scenario, 2000-2030 [11].....	7

CHAPTER 2: Previous investigations

Figure 2.1: The practical implementation of the novel VAWT.....	9
Figure 2.2: Preliminary results from field-testing of the turbine where C_p is the coefficient of performance and λ is the tip speed ratio. The dashed line is the predicted efficiency of the turbine at 10m/s from the multiple stream tube analysis of Whitten(2002).....	10
Figure 2.3: Vane-type wind turbine (b) of four Frame (c) three frames.....	10
Figure 2.4: Torque coefficient various tip speed ratio for 3 frame wind turbine.....	11
Figure 2.5: Power coefficient various tip speed ratio for 4-frame wind turbine.....	11
Figure 2.6: Prototype of the proposed Senegal VAWT.....	12
Figure 2.7: Curves of power coefficient versus TSR under different Reynolds numbers.....	12
Figure 2.8: .Plan view of a double-multiple-stream tube analysis of the flow through a VAWT rotor.....	13
Figure 2.9: Tip speed ratio and power coefficient relationship for different inlet wind speed.....	13
Figure 2.10: The two turbines were placed in their respective frames in the assembly. A floating floor was mounted on top of the boxes.....	14
Figure 2.11: Power curves for the different configurations tested.....	15
Figure 2.12: Wind turbine model installed in the wind tunnel.....	15
Figure 2.13: Power coefficients obtained from wind tunnel tests.....	16
Figure 2.14: (a) Experimental setup (b) Close view of the proposed VAWT in test rig.....	16

Figure 2.15: Variations of power coefficient (C_p) with tip speed ratio (TSR) for various aspect ratios.....	19
Figure 2.16: Performance investigation of hybrid VAWT within wind tunnel.....	20
Figure 2.17: Experimental investigation of two hybrid VAWTs in open field conditions.....	20
Figure 2.18: Characteristic curve of the hybrid VAWT.....	21
Figure 2.19: The final assembly.....	22
Figure 2.20: Comparison between coefficient of power values for the Darrieus and hybrid turbines.....	22
CHAPTER 3 :	
Figure 3.1: fabricated quarter- circular bladed.....	24
Figure 3.2: Fabricated model of quart-circular rotor montage H (twenty bladed).....	24
Figure 3.3: complete experimental setup of the wind tunnel.....	25
Figure 3.4: Eighteen perpendicular to each other.....	26
Figure 3.5: Ten blades perpendicular to each other.	26
Figure 3.6: Experience procedure.....	26
Figure 3.7: PCE-TA 30 vane thermo-anemometer with a flexible probe.....	27
Figure 3.8: digital tachometer/optical laser and contact tachometer (dt2236b).....	27
Figure 3.9: Kimo CP 300 Pressure Transmitter.....	28
Figure 3.10: Wind Tunnel SIEMENS 2CQ5400-1DB01-1BG2.....	28
Figure 3.11: Wind Tunnel elements composite.....	28
Figure 3.12: Rotor area limits.....	29
Figure 3.13: Betz limit.....	31
Figure 3.14: Different forces distribution and rotation of VAWT.....	31
Figure 3.15: Sixteen perpendicular to each other.....	32
Figure 3.16: Ten blades perpendicular to each other.	32
Figure 3.17: V form sixteen blades.....	33
Figure 3.18: V form ten blades.....	33
Figure 3.19: A form sixteen blades.....	33
Figure 3.20: A form ten blades.....	33
Figure 3.21: A form distance and inclination blades.	34
Figure 3.22: Fifteen blades perpendicular to each other three by three.	35
Figure 3.23: Twenty blades perpendicular to each other two by two.	35
Figure 3.24: S form blades shape.	36
Figure 3.25: One in One out blades form.	3

CHAPTER 4 :

Figure 4.1: power coefficient and turbine speed of all blade H form shape.....	38
Figure 4.2: TSR and number of blade of all blade H form shape.	39
Figure 4.3: Speed turbine and wind speed of all blade H form shape.	39
Figure 4.4: pressure differential and wind speed of all blade H form shape.	40
Figure 4.5: power coefficient and Number of blade of all blades H form shape.	40
Figure 4.6: power coefficient and turbine speed of all blades V form shape.	41
Figure 4.7: TSR and Number of all blades V form shape.	42
Figure 4.8: Speed turbine and wind speed of all blade V form shape.	42
Figure 4.9: pressure differential and wind speed of all blade V form shape.	43
Figure 4.10: power coefficient and Number of blade of all blades V form shape.	43
Figure 4.11: power coefficient and turbine speed of all blade shapes A form.	44
Figure 4.12: TSR and number of blade of all blade A form shape.	44
Figure 4.13: Speed turbine and wind speed of all blade A form shape.	45
Figure 4.14: pressure differential and wind speed of all blade A form shape.	45
Figure 4.15: power coefficient and Number of blades of A form shape.	46
Figure 4.16: Power coefficient and wind speed of H 3 form.	46
Figure 4.17: Power coefficient and wind speed of H 2 form.	47
Figure 4.18: Power coefficient and wind speed of S form.	47
Figure 4.19: Power coefficient and wind speed of One in One out form.	48
Figure 4.20: designs for future experience.	50

LISTE OF TABLES**CHAPTER 3 : EXPERIMENTAL STUDY**

Table 3.1: Characteristics of ten blades perpendicular to each other.	29
Table 3.2: Characteristics of ten blades V form.	30
Table 3.3: Characteristics of ten blades A form.	31
Table 3.4: distance and inclination of A form blades.	31
Table 3.5: Characteristics of Fifteen blades perpendicular to each other three by three.....	32
Table 3.6: Characteristics of twenty blades perpendicular to each other two by two.....	33
Table 3.7: Characteristics of S form blades.	33
Table 3.8: Characteristics of One in One out blades form.	34

CHAPTER 4 : RESULTS AND DISCUSSION

Table 4.1: highest values of power coefficient for all shapes.....	45
---	-----------

TABLE OF CONTENTS

DEDICATION	I
ACKNOWLEDGEMENTS	II
LIST OF SYMBOLS	III
LIST OF FIGURES	IV
LIST OF TABLES	VII

INTRODUCTION

CHAPTER 1 : Wind energy

INTRODUCTION	1
<i>1.1 Alternative Energy</i>	<i>1</i>
<i>1.2 Wind Energy.....</i>	<i>1</i>
<i>1.3 Wind Turbine and Types</i>	<i>2</i>
<i>1.4 Vertical Axis Wind Turbines</i>	<i>3</i>
<i>1.5 Characteristic</i>	<i>5</i>
<i>1.6 Applications of VAWT</i>	<i>6</i>
<i>1.7 Wind Energy Utilization</i>	<i>7</i>
<i>1.8 Objectives of the Research</i>	<i>8</i>
<i>Conclusion</i>	<i>8</i>

CHAPTER 2 : Previous investigations

<i>Introduction.....</i>	<i>9</i>
<i>2.2 Different numerical and experimental Investigations</i>	<i>9</i>
<i>Conclusion</i>	<i>19</i>

CHAPTER 3 : Experimental study

<i>Introduction</i>	21
<i>3.1 Background Research</i>	21
<i>3.2 Design turbine blade</i>	21
<i>3.3 Model structure combination</i>	22
<i>3.4 Experimental study</i>	23
<i>3.5 Measurement instruments</i>	24
<i>3.6 Measured Characteristics</i>	27
<i>3.7 Experimental studies</i>	30
<i>Conclusion</i>	35

CHAPTER 4 : Results and discussion

<i>Introduction</i>	37
<i>Results and discussion</i>	37
<i>4.1 H form VAWT</i>	37
<i>4.2 V form VAWT</i>	40
<i>4.3 A form VAWT</i>	42
<i>4.4 H 3 form VAWT</i>	45
<i>4.5 H 2 form VAWT</i>	45
<i>4.6 S form VAWT</i>	46
<i>4.7 One in One out form VAWT</i>	46
<i>Conclusion</i>	47

CONCLUSION

REFERENCE

INTRODUCTION

Due to necessity of reducing pollution, emissions and make wind energy more competitive with other production methods. Most developed countries has being using it to replace the consumption of those types of nonrenewable resources.

Vertical Axis Wind Turbine (VAWT) needs low wind speed and can be installed anywhere which are some of the reasons for this research.

The main objective of this research is to improve the design and performance of VAWT to make it more attractive, efficient, durable and sustainable. For a VAWT the blades perform the main role to extract energy from the wind.

Furthermore, almost all of the components of VAWT requiring maintenance are located at the ground level, facilitating the maintenance work appreciably. a disadvantage is that some designs are not self-starting.

In general, VAWT can sensibly be used in any area with sufficient wind.

CHAPTER

1

CHAPTER 1

Introduction

Energy demand is creeping up every day, every year due to increase of population, industrial and agricultural advancement in the world, this related of globalization and technology Which assure the improvement of this world, but the conventional energy sources are becoming limited according to increases in energy consumption, which stimulate the humanity to find the alternative sources of energy.

1.1 Alternative Energy

Alternative sources involve natural phenomena such as sunlight, wind, tides, plant growth, and geothermal heat. Solar and Wind power are the most popular among the various sources of renewable energy. If the whole world unites, develops and benefits these two kinds of alternative sources that can generate most of the world's electricity for years and help the climate change condition.

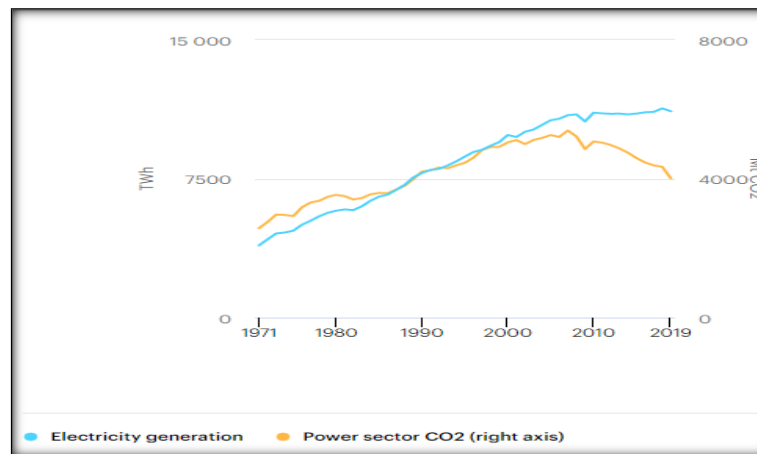


Figure 1.1: Electricity generation and power sector CO2 emissions in advanced economies, 1971-2019 [1]

1.2 Wind Energy

The wind is a clean, free, and readily available renewable energy source. Each day, around the world, wind turbines are capturing the wind's power and converting it to electricity. Wind power generation plays an increasingly important role in the way we power our world – in a clean, sustainable manner. Wind power is one of the fastest-growing energy sources in the world because of its many advantages. Wind power also presents inherent challenges in some regions of the world, which are being addressed through research and development (R&D) projects around the globe. [2]

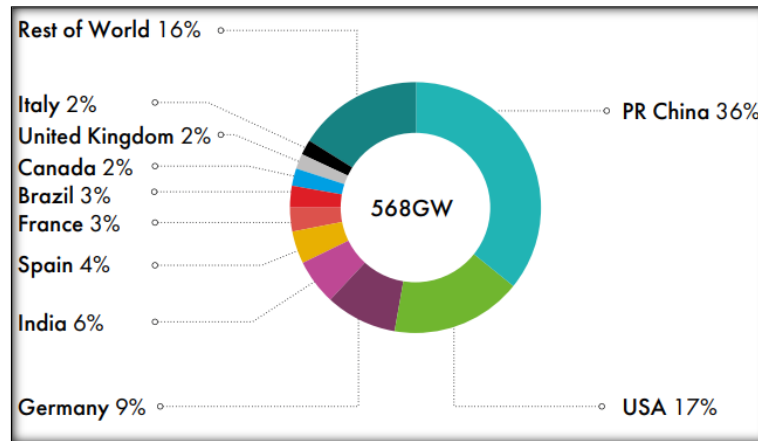


Figure 1.2 : Total installations onshore [13]

The disadvantages are its lower efficiency and high installation cost. But the ultimate cost would be lowered if it operates continuously and small scale turbines can be installed in any corner of the world.

1.3 Wind Turbine and Types

Wind turbines are usually used to convert the wind kinetic energy into electrical power. According to the alignment of rotational axis, wind turbines can be categorized into two main types: horizontal-axis wind turbines (HAWTs) and vertical-axis wind turbines (VAWTs). Currently, most of the commercial wind turbines are deployed as horizontal-axis configurations because HAWTs are more efficient at large scales and have a longer lifetime in comparison to VAWT designs. However, VAWT designs possess several prominent advantages over HAWT configurations, such as insensitive to wind direction, easy to install and maintain, lower noise emission and less dangerous to birds. VAWTs offer a safer, more convenient and economical solution for wind energy harvest in the urban, suburban and rural environments, such as top of buildings and backyards. Furthermore, as we know that the wind speed in these areas is relatively low and highly turbulent, while VAWTs require a lower wind speed to self-start, which makes them a good candidate to harness wind energy in the areas with relatively insufficient wind resources.[3]

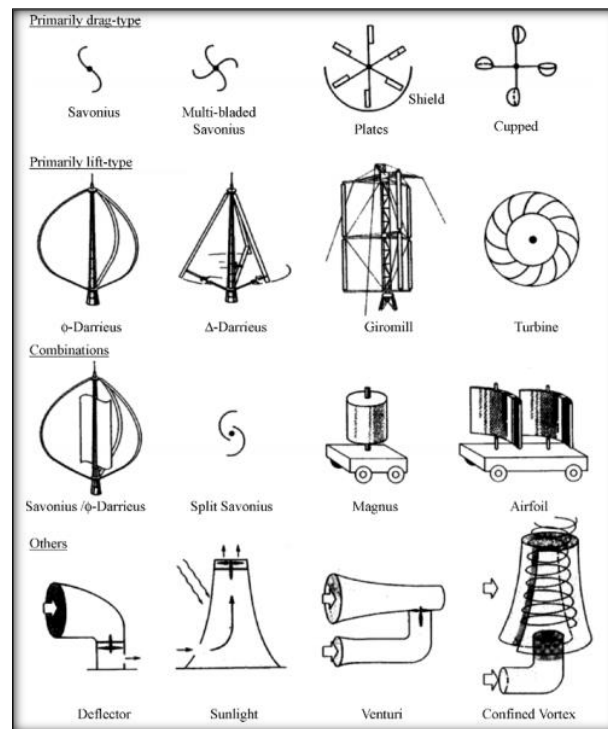


Figure 1.3: Various concepts for vertical axis turbines (Eldridge, 1980) [15]

1.4 Vertical Axis Wind Turbines

From history book, it was found that about 1300 A.D a Syrian cosmographer Al-Dimashqi drew a vertical axis windmill (Shepherd 1990). It was a two storied wall structure with milestones at the top and a rotor at the bottom. It had latter with spoked reel with 6 to 12 upright ribs that covered with cloth. It was found that this type of windmill had been in operation in 1963 which used to produce an estimated 75 hp (at efficiency of 50% at wind speed 30 m/s). Each windmill milled one ton of grain per day (Wulff 1966).[6]

In general, VAWT is driven by two types of forces of wind, drag and lift force. Savonius rotor is the simplest kind of VAWTs is a drag-type configuration and a bit complex type is Darrieus rotor which is lift-type configuration.

Savonius Rotor:

The Savonius wind turbine was first used by a Finnish Engineer S. J. Savonius in 1931 (Savonius 1931). The design of his rotor was S-shaped with two semi-circular buckets with small overlap. At that time this rotor was successfully used as an ocean current meter

The operation of Savonius rotor depends on the difference of drag force when the wind strikes the concave and convex part of the semi-spherical blades. The flow energy utilization of Savonius rotor is lower than that of Darrieus rotor. Hence this type of turbine is generally not used for high-power applications and usually used for wind velocimetry applications (Islam, Ting and Fartaj 2008). The greatest advantage of a Savonius rotor is its ability to self-start in contrast to other 'Lift type' VAWTs (Mohamed, et al. 2011). Recently, some generators with high torque at low rotational speed, suitable for small-scale wind turbines, have been developed, suggesting that Savonius rotors may yet be used to generate electric power (T. Hayashi, et al. 2004).

[6]

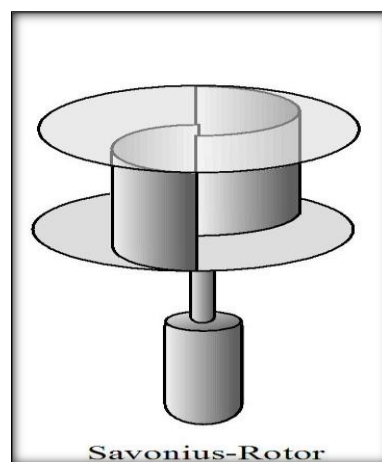


Figure 1.4: Savonius rotor [7]

Darrieus Rotor:

In 1931, G. J. M. Darrieus in France patented another VAWT named Darrieus vertical axis rotor. This type of rotor was not self-starting.

The energy is taken from the wind by a component of the lift force working in the direction of rotation. Lift force is perpendicular to the resultant of two velocity component of wind velocity and relative velocity of airfoil to the shaft. These types of turbines have highest values of efficiency among VAWTs and the tip speed ratio can be much higher resulting in a much higher rpm. But generally suffer from problems of low starting torque and poor building integration.[6]

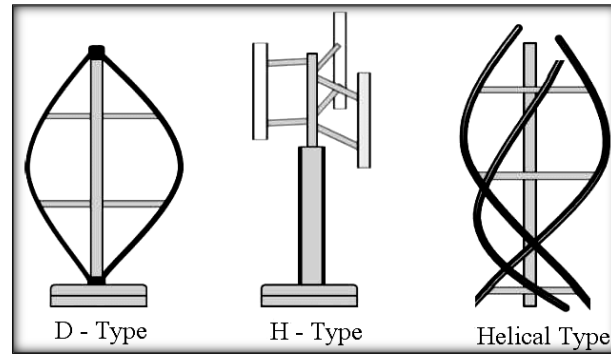


Figure 1.5: Different types of Darrieus rotor [8]

Combined Savonius and Darrieus Rotor:

Since the Darrieus rotor is not self-starting; a blended design with Savonius blade can make the hybrid which can make it starting and more efficient than any of the single rotor. [6]

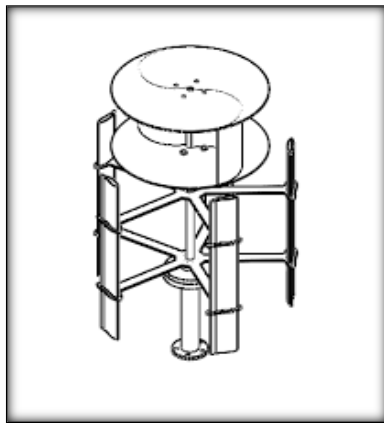


Figure 1.6: Combined Savonius and Darrieus Rotor [9]

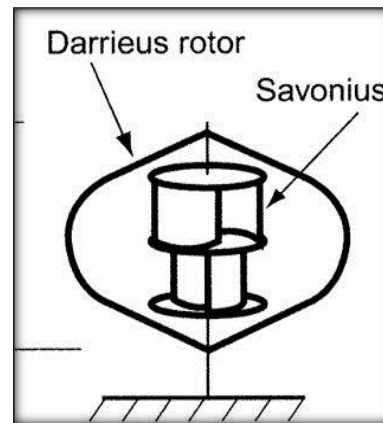


Figure 1.7: Combined Savonius and Darrieus Rotor [9]

1.5 Characteristic:

- **Savonius rotor:** [14]

1. Self-Starting
2. Low Speed
3. Low Efficiency
4. Torque is produced by pressure difference between two-sides of the half facing the wind.
5. It needs a large surface area.

- **Darrieus rotor:** [14]

1. Not Self-Starting
2. High Speed

3. High Efficiency
4. Potentially Low Capital Cost.
5. It needs much less surface area.

1.6 Applications of VAWT [14]

- Vertical Axis Wind Turbine or better abbreviated as VAWT successfully finds application in many areas ranging from power generation to power lamps. These are described in few details in the following points below:

- Power Generation: - It is quite known and common that wind turbines have been used for power generation throughout the world. They are commercially available for electricity generation.
- Water Pumping: VAWT have used as mechanical application for pumping of water.
- In Telecommunications/Grid Monitoring: VAWT or Vertical Axis Wind Turbine are gaining wide popularity in the field of telecommunications since they are used for monitoring of mobile stations in Korea ,China ,etc. Other countries.
- Wind & Solar Lamps: - Wind solar hybrid system for parking lot, etc. are being developed in various countries like Japan, etc. and their usage is mostly based on VAWT.
- Polar Research Station System: - VAWT have found their usage in Antarctica as for generation of power supply.
- Energy Recovery Systems: - There have been various researches going on throughout the world where VAWT are used as systems that are helpful in recovering energy.
- Increase in Power Generation System: - VAWT are used as substitute for gaining more power generation etc.

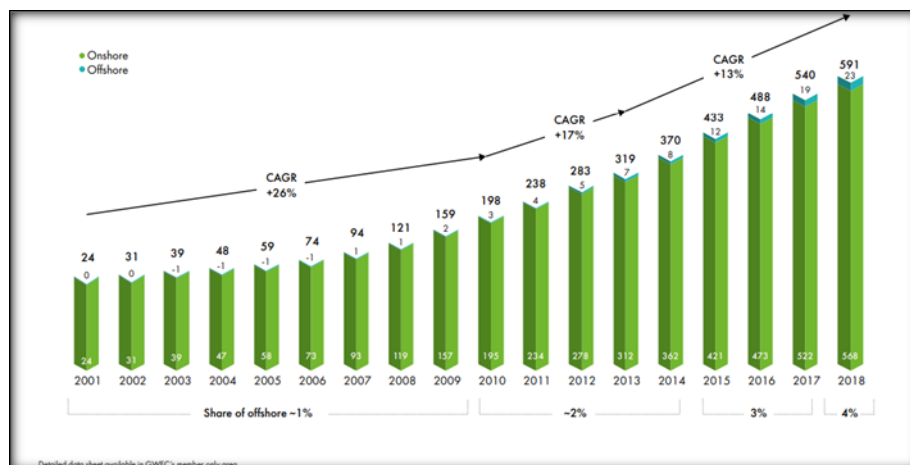


Figure 1.8: Historic development of total installations [13]

1.7 Wind Energy Utilization

Energy from wind can be harnessed in several forms. It could be used to run turbines and hence produce electricity, provide mechanical power, run wind pumps, propel sails or could be simply just used for drying or husk separation in agriculture. The most common, widespread and perhaps economically significant among these is the use of wind energy to produce power in wind farms. Wind energy is progressively being used as a means to reduce the dependency on non-renewable energy sources. Furthermore, its use can be advocated as it comes with no environmental pollution and is not likely to ever run out. [10]

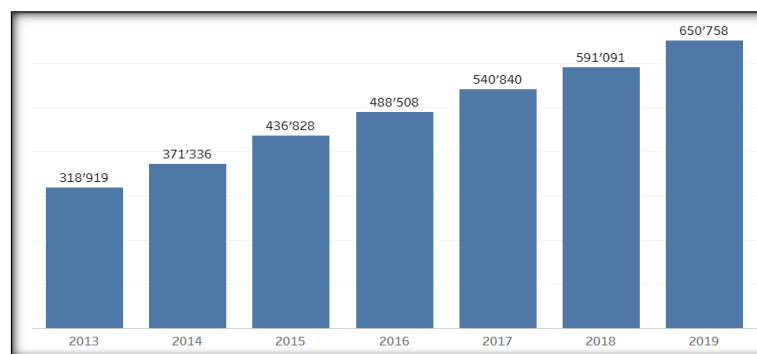


Figure 1.9 : Total Installed Capacity [MW] [12]

In 2018, onshore wind electricity generation increased by an estimated 12%, while capacity additions only grew 7%. However, more efforts are needed: annual additions of onshore wind capacity need to increase much faster through 2030 to get on track with the Sustainable Development Scenario.[11]

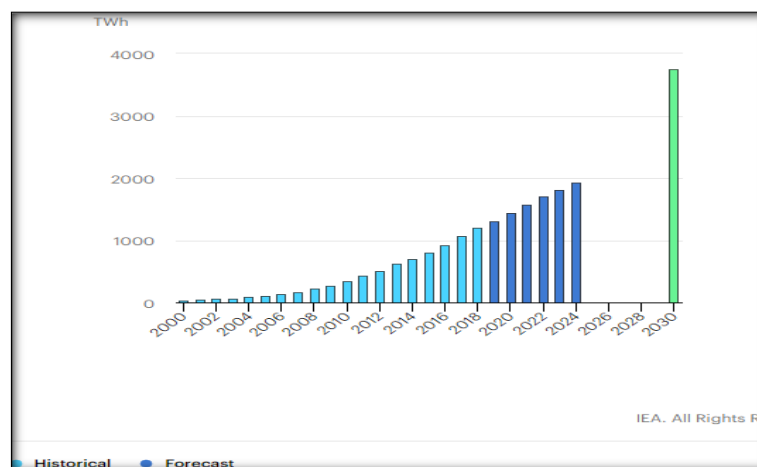


Figure 1.10: Onshore wind power generation in the Sustainable Development Scenario, 2000-2030 [11]

1.8 Objectives of the Research

The objective of this research is to find the highly efficient VAWT by modeling a form of the blades of Darrius rotor. In order to investigate the improvement of the performance the following steps were set for the research:

- To design and fabricate Darrius rotor wind turbine with optimum blade numbers and selected shapes;
- To create a Fluid flow field around the models using wind tunnel SIEMENS 2CQ5400-1DB01-1BG2 for study; at various wind speed then to find, power coefficient, pressure contours, TSR, rounds number of turbine .
- To calculate the numerical power coefficient using equation (6)
- After finding the results we compare all experimental results shapes and make a conclusion.

Conclusion:

According to previous information about wind energy, it's a necessary to develop and encourage wind power energy utilization because of economics and positives for nature and energy saving.

CHAPTER 2

CHAPTER 2

Introduction

Vertical-axis wind turbines (VAWTs), which are considered an important wind energy conversion device, have recently received renewed attention.

Researchers have been trying their best to find the best form rotor. Meanwhile. These researches are numerical and theoretical prediction for blades shape, characteristics and flow around the wind turbines and from that it varies from research laboratories to full scale simulation. The extensive amount of work has been carried to improve the wind energy utilization efficiency of VAWTs and find a sustainable solution. Around the globe researchers have been experimenting on HAWT and Darrieus rotor for large scale energy production and Savonius rotor for small scale usage. There is some investigations.

2.2 Different numerical and experimental Investigations:

- **WOLLONGONG TURBINE:**

The prototype of the Wollongong Turbine was installed at the University of Wollongong Engineering Innovation and Education Centre .A number of preliminary tests have been carried out on the device, which has operated successfully. In particular, the device has a very strong torque characteristic at low tip speed ratio, which means it is self-starting and may lend itself to applications such as water pumping. In addition, the rotor generates very little aerodynamic noise due to the low blade tip speeds..[16]



Figure 2.1: The practical implementation of the novel VAWT. [16]

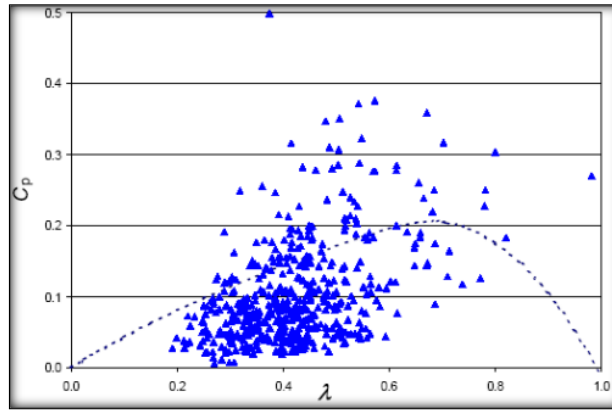


Figure 2.2: Preliminary results from field-testing of the turbine where C_p is the coefficient of performance and λ is the tip speed ratio. The dashed line is the predicted efficiency of the turbine at 10m/s from the multiple stream tube analysis of Whitten (2002). [16]

Preliminary tests have confirmed that device does indeed self-start with a high torque and power in a tip speed range of between 0.2 and 0.8. Further testing is required to confirm these initial tests. The project has proven to provide very successful training in wind energy for engineering undergraduate students. [16]

- **VANE WIND TURBINE:**

The proposed vane type vertical wind turbine can be designed by two types of construction. The first is four frames with angles of 90° to each other and horizontally constructed bars with vanes that have ability to twist on 90° . The second is three frames with angles of 120° between each other. Increase the number of frames will not increase efficiency of the wind turbine because increases the vane inter frame wind shadow area and increases the weight of turbine. [17]

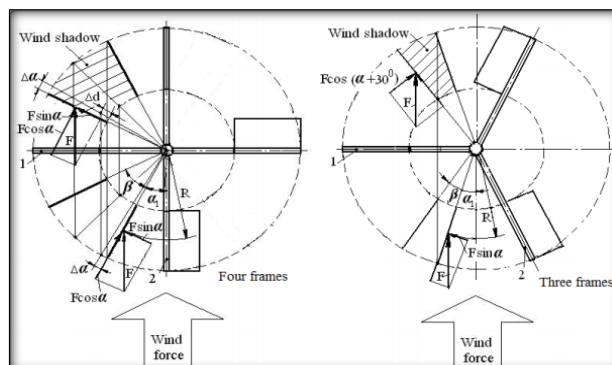


Figure 2.3: Vane-type wind turbine (b) of four Frame (c) three frames. [17]

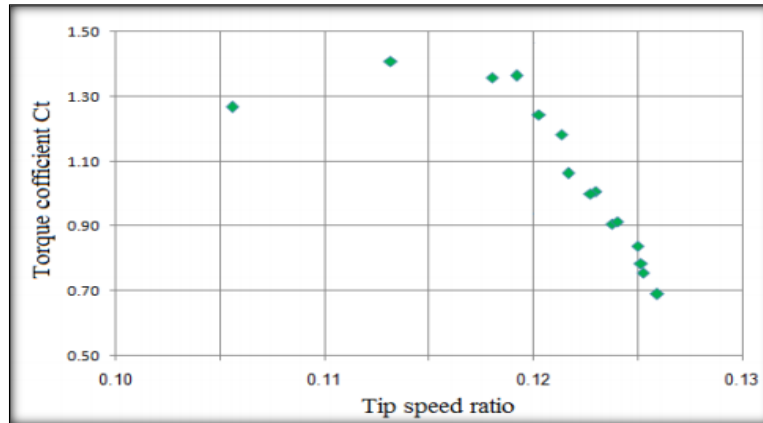


Figure 2.4: Torque coefficient various tip speed ratio for 3 frame wind turbine. [17]

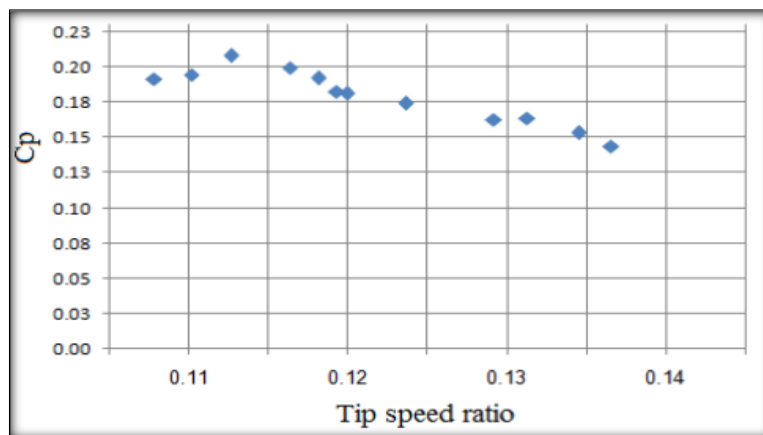


Figure 2.5: Power coefficient various tip speed ratio for 4-frame wind turbine. [17]

Based on the results of experiments, the results satisfy the theoretical approach (Eqs. 5-9). The four-frame wind turbines have a higher efficiency compared to the three-frame turbine. This is because the four-frame wind turbines have more area to capture wind energy. The rotation speed of the wind turbine with the dynamo shows a small drop of the turbine speed without dynamo at the same wind velocity. Both test models had exposure in the same condition of wind speed by wind tunnel. Results show that the coefficient of performance and hence the efficiency of the vane-type wind turbine are decreasing with an increase in wind speed. The vane-type turbines show the higher efficiency at the low wind speed. This type of wind turbine has good technical properties and can be used for generating a power more efficiently for the low speed of the wind. [17]

- **DRAG-TYPE VAWT:**

This article investigates a Senegal drag-type VAWT under different configurations to find an optimal design that has the characteristics of low cut-in speed, high power density, and robustness to adjacent objects.[18]



Figure 2.6: Prototype of the proposed Senegal VAWT.[18]

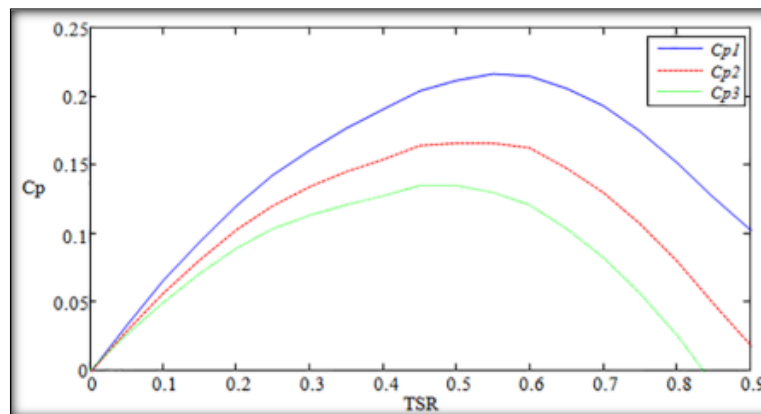


Figure 2.7: Curves of power coefficient versus TSR under different Reynolds numbers.[18]

Curves of C_p versus TSR under different wind speeds, where the Res are set at 490,000(C_{p1}), 670,000 (C_{p2}), and 890,000 (C_{p3}), respectively. It can be found from Figure 7 that the wind energy utilization rate first increases and then decreases with the increase of TSR. The maximum value occurs when the TSR is between 0.5 and 0.6.[18]

- **DOUBLE MULTIPLE STREAM TUBE (DMST) MODEL:**

In this section the simulation model is assumed to be the Double Multiple Stream Tube (DMST) Model. This model is a combination of the MST model and double actuator theory [17], where the turbine is modeled separately for the upwind half and the downstream half. Also an assumption is made that the wake from the upwind pass is fully expanded and the ultimate wake velocity has been reached before the interaction with the blades in the downwind pass. Fig. 1 presents the DMST model diagram. Each airfoil in this model intersects each stream tube twice, one on the upwind pass and the other on the downwind pass. The DMST model solves two equations simultaneously for the stream-wise force at the actuator disk; one obtained by conservation of momentum and other based on the aerodynamic coefficients of the airfoil (Lift and Drag) and the local wind velocity. These equations are solved twice, one for the upwind part and the other for the downwind part. Fig. 2 shows the forces and velocities triangles acting on the turbine un-pitched blade.[19]

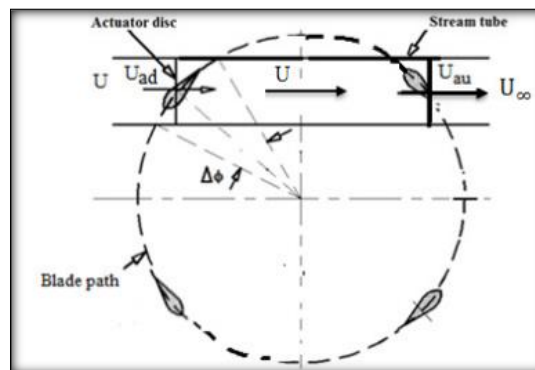


Figure 2.8: .Plan view of a double-multiple-stream tube analysis of the flow through a VAWT rotor.[19]

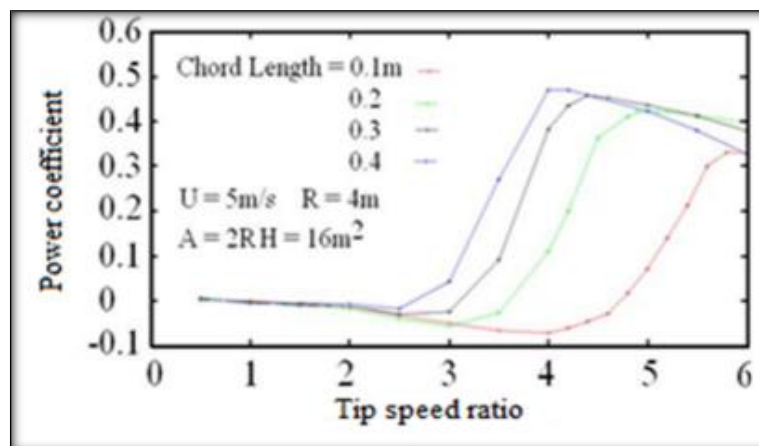


Figure 2.9:Tip speed ratio and power coefficient relationship for different inlet wind speed.[19]

The DMST model developed in this work was checked against the vertical axis wind turbine using CFD model which was introduced by Biadgo et al. [19]. The computer program used in this work is fitted by the same data used in [19], since the normal NACA0012 airfoil was set to 0.2 m chord length and the turbine radius was set 2 m. The height of turbine is taken to be 4 m with 3 blades. The wind speed used is 5 m/s and tip speed ratios are 0.25, 0.5, 1, 2, 3, 4, 5, 6, and 7, the total number of stream tubes is 12 with $\Delta\Phi = 15^\circ$. The computational proceeding was applied to DMST model and the first aspect of the model validation is the comparison of the predicted VAWT power coefficient (C_p) for different tip speed ratio λ as shown in Fig. 15. In this figure the relation between power coefficient and tip speed ratio is graphed for the DMST model introduced by the present work and the results obtained by [19] for both DMST and CFD model. [19]

- **TWO-BLADED H-TYPE DARRIEUS TURBINE:**

The rotor is a two-bladed H-type Darrieus turbine with two NACA 0018 blades and two inclined struts per blade. The struts are slightly thicker (NACA 0024) for structural reasons. The rotor solidity, $s = \frac{1}{4} bc = D$, is 0.20, where b is the number of blades and D the rotor diameter. The chord length, c , is 50 mm. Fig. 1 shows the rotor and the setup with the rotor diameter and height, H , indicated with their respective symbol. [20]



Figure 2.10: The two turbines were placed in their respective frames in the assembly. A floating floor was mounted on top of the boxes. [20]

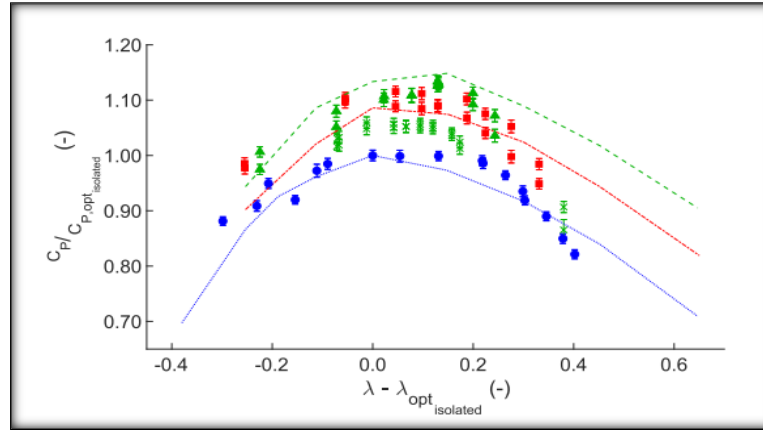


Figure 2.11: Power curves for the different configurations tested. [20]

Wind tunnel experiments have been used to analyse the performance of a pair of two H-type Darrieus VAWTs placed side-by-side in close vicinity in a plane normal to a uniform inflow. For small inter-turbine distances (1.2 and 1.3 times the rotor diameter), we observed a power increase of up to about 16% for a pair of VAWTs compared with two individual VAWTs. Apart from the distance between the turbines, the power increase also depends on the tip-speed ratio and the direction of rotation. The power coefficients have been rescaled with the maximum CP of the isolated turbine, while the tip-speed ratios have been shifted to set the tip-speed ratio corresponding to the maximum CP at zero. A number of interesting conclusions can be drawn from this comparison. [20]

- **HIGH-SOLIDITY STRAIGHT BLADED VERTICAL AXIS WIND TURBINES(HIGH-SOLIDITY SBVAWTS):**

A high-solidity variable-pitch SBVAWT with three blades, a blade chord length of 0.3 m, a radius of 1 m, a blade length of 1.5 m, and a solidity of 0.45 (solidity $\delta = Nc/D$) was designed and manufactured, as shown in Fig. 9. The blade was made of foam covered by glass fiber reinforced plastic of a thickness of 0.7 mm as a shell. The blade used in this study has a smooth surface, and the blade surface roughness will not be considered in this study.[21]



Figure 2.12: Wind turbine model installed in the wind tunnel.[21]

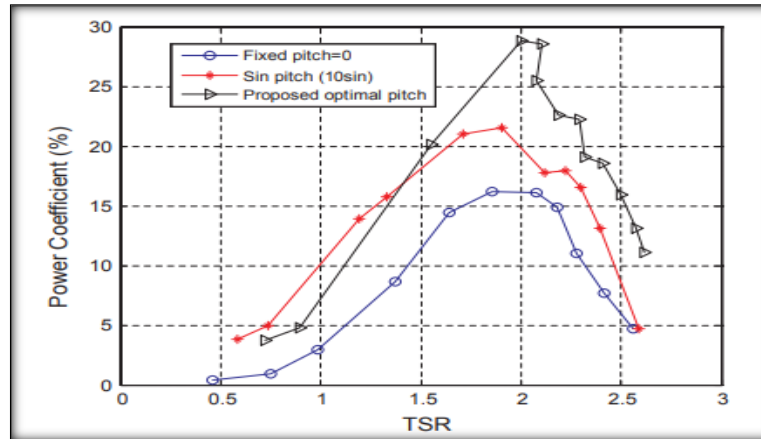


Figure 2.13: Power coefficients obtained from wind tunnel tests.[21]

The power coefficient C_p was calculated by Eq. (21). Fig. 21 shows the test results of the power coefficients. It can be seen that both the proposed optimal pitch function and the sinusoidal pitch function substantially increased the power coefficients compared with the fixed-pitch case. Furthermore, the proposed optimal pitch function provided more power to the high-solidity SBVAWT than the sinusoidal pitch function within the TSR range from 1.5 to 2.5. The measured maximum power coefficient of the wind turbine with the proposed optimal pitch function increased by 78.6% compared to the fixed-pitch case, while the sinusoidal pitch case made enhancement of 33.2% at the measured maximum point, compared with the fixed-pitch case. [21]

- **H-ROTOR WITH SEMI-ELLIPTIC SHAPED BLADED VERTICAL AXIS WIND TURBINE:**

The experimental investigation is carried out to obtain the data set for analyzing the performance of this non-conventional H-rotor with semi-elliptic shaped bladed vertical axis wind turbine by varying the aspect ratio (H/D) at low-wind speeds which is varied from 3 m/s to 6 m/s. The aspect ratio is varied from 1.0 to 1.22 in this present study.[22]



Figure 2.14: (a) Experimental setup (b) Close view of the proposed VAWT in test rig. [22]

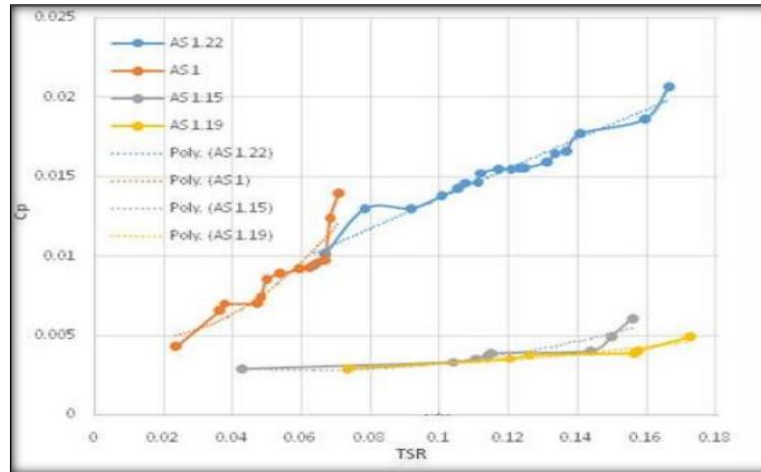


Figure 2.15: Variations of power coefficient (C_p) with tip speed ratio (TSR) for various aspect ratios. [22]

During experimentation, it is observed that the VAWT has the self-starting characteristics and it tends to rotate even at low-wind speed regimes. The coefficient of power reached the maximum value for an aspect ratio of 1.22. The power coefficient has reached its maximum value of 0.0207 with a TSR value of 0.1667 at a wind velocity of 5.54 m/s. [22]

- **HYBRID ALUMINUM-ALLOY VAWT:**

A hybrid aluminum-alloy VAWT of 1.09 m (H) x 1.23 m (W), which is coupled with a three-phase AC generator of 300 W at a rated wind speed of 15 m/s, is mounted within a wind tunnel of 2.4 x 2.4 x 3.6 m³ for the experimental investigation of mechanical performances. Fig. 2 shows an experimental apparatus for investigating the mechanical performances of a hybrid VAWT within a wind tunnel. The hybrid VAWT has a uniform airflow at different wind speeds to obtain the characteristic curve of power coefficients vs. tip speed ratios. For a given wind speed [23]



Figure 2.16: Performance investigation of hybrid VAWT within wind tunnel.[23]

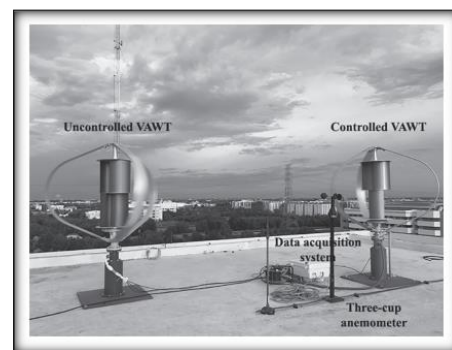


Figure 2.17: Experimental investigation of two hybrid VAWTs in open field conditions.[23]

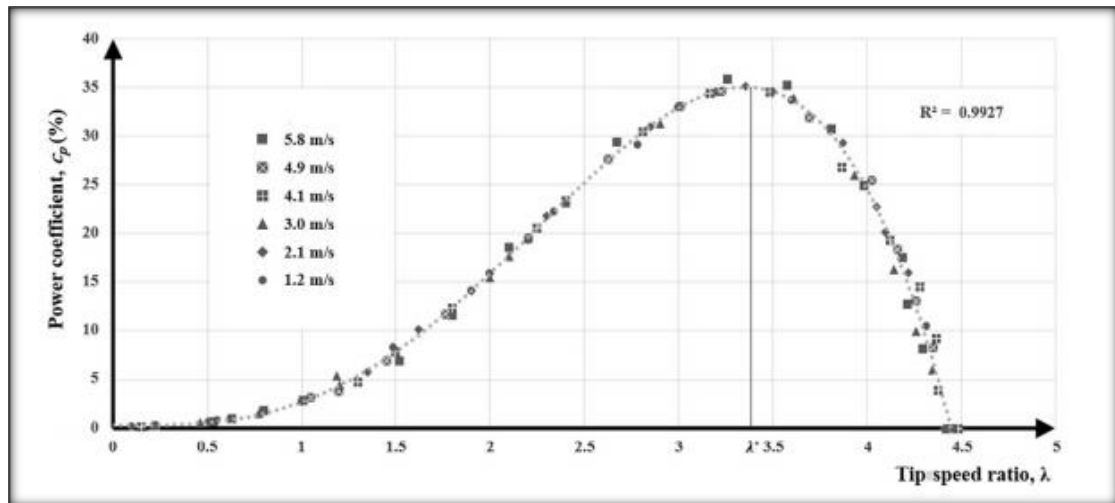


Figure 2.18: Characteristic curve of the hybrid VAWT.[23]

The obtained characteristic curve shows the performance of the Darrieus VAWT where the high power coefficients are at a high tip speed ratio (greater than unity) while the power coefficients are typically null at a low tip speed ratio. However, Savonius VAWT increases the power coefficients of the hybrid VAWT from null values at low tip speed ratios. The optimal tip speed ratio is 3.4 where the maximum value of the power coefficient is 35%. For this hybrid VAWT, the rotation is expected to be managed at this optimal tip speed ratio to yield maximum mechanical works in a wide range of wind speeds over time.[23]

- **COMBINED BACH-TYPE AND H-DARRIEUS ROTOR SYSTEMS:**

Hybrid VAWTs can be a combination of drag-based and lift-based rotors such as the Savonius and Darrieus turbines, respectively. This combination can address the drawbacks of each turbine design, as mentioned above, such as obtaining self-starting characteristics at low λ values and high C_p at high λ values [15]. However, hybrid VAWTs have certain challenges such as new forms of vortex shedding, more complex system design optimization, and relatively lower performance due to the created drag forces by the Savonius turbine at high λ values.[24]

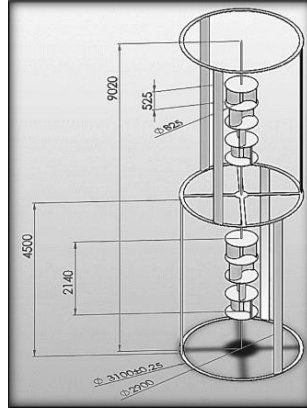


Figure 2.19: The final assembly.[24]

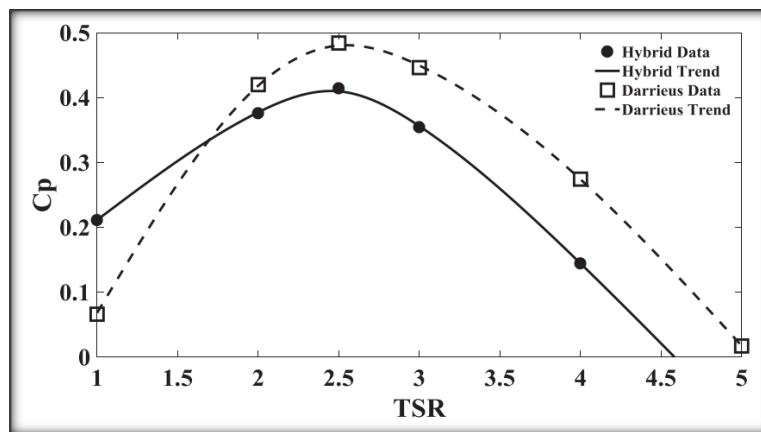


Figure 2.20: Comparison between coefficient of power values for the Darrieus and hybrid turbines.[24]

C_p trends and numerical values for studied Darrieus and hybrid VAWTs. As noted, when compared with the Darrieus turbine, the immense drag force from the Bach turbine at high TSRs reduces the moment on the hybrid turbine and therefore, this turbine has lower maximum C_p and lower maximum operation TSR. Bhuyan et al. [15] also reached similar conditions with their hybrid VAWT design. On the other hand, this turbine does not require start-up mechanisms and uses the Bach rotor system to start its operation.[24]

Conclusion:

Based on experimental investigations results and conclusions. VAWT type, number of blades and wind speed from factors, which make a turbine work in high performance. According to this information, we try to create and develop a VAWT from cheap materials with many shapes in order to improve the performance.

CHAPTER

3

CHAPTER 3

Introduction

The research objective is to find the highly efficient Vertical Axis Wind Turbine by studying the characteristics shapes of quarter-circular blades of Darrius rotor from cheap, efficient and available materials. . To accomplish this goal, the objectives were to combine the montage prototype of blades and some tests were conducted in front of a subsonic wind tunnel varying the wind speed. Wind speed and rotational speed are measured and used to calculate angular velocity, Reynolds number, tip speed ratio and power coefficient.

To come across these objectives, the tasks were to:

- Complete background research on wind turbine data
- Design turbine blade designs for testing
- Model structure combination
- Manufacture parts and build the model for experimental set up

3.1 Background Research:

Background research included reviewing previous projects, Which provided a foundation for the current project. Using that information, we then studied new designs in order to complete our research.

Analysing previous researches and articles like Computational and Experimental Study on Vertical Axis Wind Turbine in Search for an Efficient Design, by Mohammad M. Bashar, Vertical Axis Wind Turbine Evaluation and Design, by Lucas Deisadze, Drew Digeser, Christopher Dunn and Dillon Shoikat. Allowed us to Diversification of shapes to find the highly efficient Vertical Axis Wind Turbine.

3.2 Design turbine blade:

After compiling background research, we decided to design a quarter-circular blade in figure 3.1 that could be tested to demonstrate improved results. Blades and the corresponding models were manufactured manually with available machines in the technological hall. This blade model was made of galvanized steel of diameter, $d = 0.8$ m, and height, $H = 0.6$ m.



Figure 3.1: fabricated quarter- circular bladed.

3.3 Model structure combination:

Based on recent researches, various VAWT models were designed and manufactured like savonius and hybrid models. We choose a VAWT The blades turbine were made of galvanized steel and with a central shaft of hard steel with a diameter of 0.8 cm to avoid twisting. The blades were 18° apart from each other and the overall rotor diameter was $D = 60$ cm. The two discs holding the blades were made of Lightwood. The quarter- circular model was made of twenty quarter-cylindrical blades of diameter, $d = 8.1$ cm, and height, $H = 60$ cm. degree and distance between blades changes from shape to another.



Figure 3.2: Fabricated model of quart-circular rotor montage H (twenty bladed).

During the testing procedure, these rotor models were placed in front of the tunnel, at 2 metres downstream from the outlet to ensure a uniform wind flow. The models were placed around vertical axes of the cross section. These blade models were able to rotate freely around the shaft supports with chains tensioners to assure a free rotation and solid fixation.



Figure 3.3: complete experimental setup of the wind tunnel.

3.4 Experimental study:

The experiment was carried out on fluid mechanics laboratory in the technological hall of the Department of Mechanical Engineering at the University of Biskra. The tests done during the period of the month of February and March 2020.

A subsonic wind tunnel with the capacity to change the wind speed is considered to produce wind velocity. The experiment needs to be done under different wind velocity. Different blade shapes combination is created to compare results. The airfoil SIEMENS 2CQ5400-1DB01-1BG2 series is chosen to create airfoil.

In this experience, we chose 20 blades assembly as the first assembly, then we use 18, 16, 14 and 10 blades assembly. The blades are placed in different shapes, angles and distances from each other and from the axis. The whole turbine model assembly installed in a frame. Air is the only fluid for the experiment. The models are tested using the interchangeable design varying wind speed of the airfoil. This wind speeds produce different angular speed of the rotor and the torque. Based on same base load, the torque is measured and angular speed is measured manually. The effect of temperature can be ignored in this measurement technique as the experiment is carried out at atmospheric temperature. For the regular room temperature 35° the air density $\rho = 1.145 \text{ kg/m}^3$ and air kinematic viscosity $\nu = 1.655 \cdot 10^{-5} \text{ m}^2/\text{s}$.

There is some models we combined to study their efficient:



Figure 3.4: Eighteen perpendicular to each other.



Figure 3.5: Ten blades perpendicular to each other.

The experiments were carried out at many different wind speeds from 2 to 15 m/s. Wind speeds were measured by a handheld anemometer at different locations at a distance of 1.5 metres from the VAWT rotor. The average wind velocity around the rotor was taken into account while doing the calculations. A plate support was fabricated that held the sensors of pressure in a location that allowed for smooth couplings and easy rotation. The rotational speed of the rotor (N) was measured by a non-contact handheld photo tachometer.



Figure 3.6: Experience procedure.

3.5 Measurement instruments:

- **Speed measurement:**

The propeller thermo-anemometer can measure air speed, air temperature and flow. The PCE-TA 30 (Figure 3.7) propeller thermo-anemometer can be used immediately and clearly indicates the measurement values on the large screen, which has background illumination. The device makes it possible to maintain the current value on the screen and to indicate the minimum and maximum values. The flexible probe of the propeller thermo-anemometer, with a length of 40 cm, allows you to measure in places with difficult access or in slightly distant ventilation channels.



Figure 3.7: PCE-TA 30 vane thermo-anemometer with a flexible probe.

- **Rotation measurement:**

A tachometer is used to measure the speed of rotation. This tachometer works by contact and with lasers. The measurement taken in direct contact (or without contact with the laser) with the device and reads the RPM and the linear surface speed.



Figure 3.8: digital tachometer/optical laser and contact tachometer (dt2236b).

- **Pressure measurement:**

Kimo instruments, class 300 transmitters have 2 analogue outputs which correspond to the first 2 parameters displayed. You can activate 1 or 2 outputs, and for each output, you can choose between pressure, temperature (probe in options), airspeed and airflow (optional functions).



Figure 3.9: Kimo CP 300 Pressure Transmitter

- **Subsonic Wind Tunnel:**

The wind tunnel is used to minimize the effects of turbulence, to maintain the stable airflow, and also to produce the homogeneous airflow. The wind tunnel is applied to achieve the wind sensor characteristics, and to verify the experimental results.



Figure 3.10: Wind Tunnel SIEMENS 2CQ5400-1DB01-1BG2:

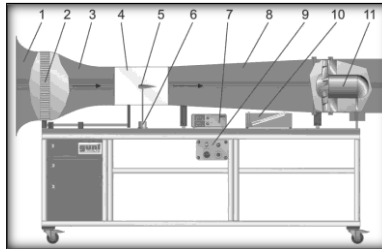


Figure 3.11: Wind Tunnel elements composite.

1-inlet contour	2-flow straightener	3-nozzle	4-measuring section	5-drag body	
6-force sensor	7-display and control unit	8-diffuser	9-switch cabinet	10-inclined tube manometer	11-axial fan

The subsonic wind tunnel as shown above (Figure 3.10) was 2.5 metres long and 1.5 metres high consisting a converging mouth entry, a honeycomb section at the inlet side, a fan section, a rectangle test section, a nets protection at the exit side. The airflow was generated using a variable frequency axial flow fan inside the tunnel and the air velocity was controlled using a variable frequency drive. The converging mouth entry was designed for an easy entry of air in the tunnel as well as to maintain a uniform flow through it. The first honeycomb section was used to reduce the swirling effect and make the flow straight. The exit section was used to make the flow straight and uniform.

3.6 Measured Characteristics

- **Rotor area:**

As the rotor turns, its blades generate an imaginary surface whose projection on a vertical plane to wind direction. The amount of energy produced by a wind turbine primarily depends on the rotor area, also referred to as cross-sectional area, swept area, or intercept area. The swept area for Darrius wind turbines can be calculated from the dimensions of the rotor (Figure 3.12).

The simple equation is : $A = D * H$ (1)

Where:

A: rotor area (m²)

H = the rotor height (m)

D = the rotor diameter (m)

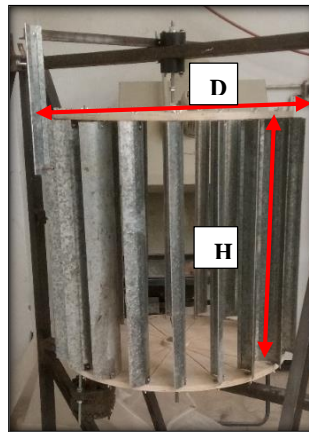


Figure 3.12: Rotor area limits.

- **The Tip speed ratio (λ):**

The tip speed ratio is the ratio of the product of blade radius and angular speed of the rotor to the wind velocity.

The Tip speed ratio (TSR) $\lambda = \omega * d / V$ (2)

Where:

ω = the angular velocity of Darrius rotor = $2 * \Pi * N / 60$ (rad/sec). (3)

d = the diameter of the rotor (m).

V = the wind speed (m/sec)

- **Power Coefficient (Cp):**

Power coefficient (Cp) of a wind turbine is the ratio of maximum power obtained from the wind to the total power available in the wind. Principally the power that the Darrius rotor can extract from the wind (Pt) is less than the actual available from the wind power (Pa). The available power (Pa), which is also the kinetic energy (KE) of the wind, can be defined as:

$$\mathbf{KE = Pa = 0.5 * ma * V^2 \text{ (Watt)}}$$

$$\mathbf{Pa = 0.5 \rho . A . V}$$

Where:

ma = wind mass flow rate striking the swept area of the wind turbine (kg/sec). = $\rho . As . V$
but, the rotor area ($A = H * D$), therefore the actual power becomes:

$$\mathbf{Pa = 0.5 \rho . H . D . V^3} \quad (4)$$

The power that the rotor extract from the wind is: $\mathbf{Pt = \Delta p * Vt * A} \quad (5)$

Where: **Pw** = the power that the rotor extracts from the wind (Watt). The power coefficient (**Cp**) is given by:

$$\mathbf{Cp = \frac{\text{extracted power from the wind}}{\text{the available power of the wind}} = \frac{Pt}{Pa}} \quad (6)$$

A German physicist Albert Betz concluded in 1919 that no wind turbine can convert more than 16/27 (59.3%) of the kinetic energy of the wind into mechanical energy turning a rotor. To this day, this is known as the Betz Limit or Betz' Law. The theoretical maximum power efficiency of any design of wind turbines is 0.59 (i.e. no more than 59% of the energy carried by the wind can be extracted by a wind turbine). This is called the “power coefficient” and is defined as: **Cp max= 0.59**

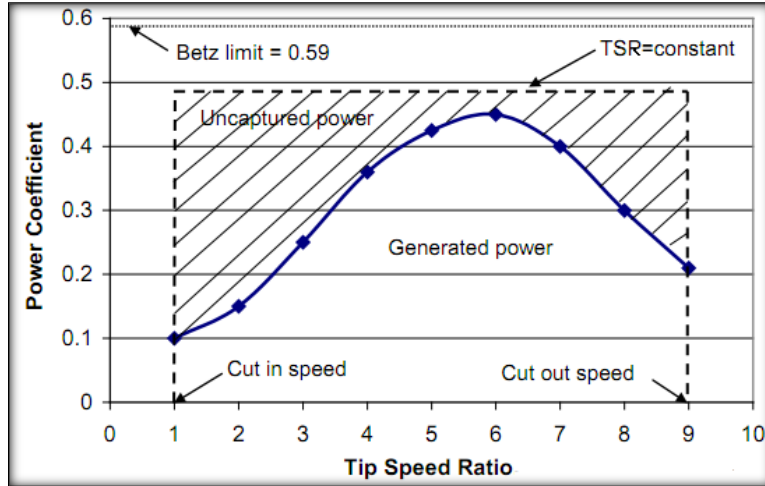


Figure 3.13: Betz limit.

- Forces and rotor direction:

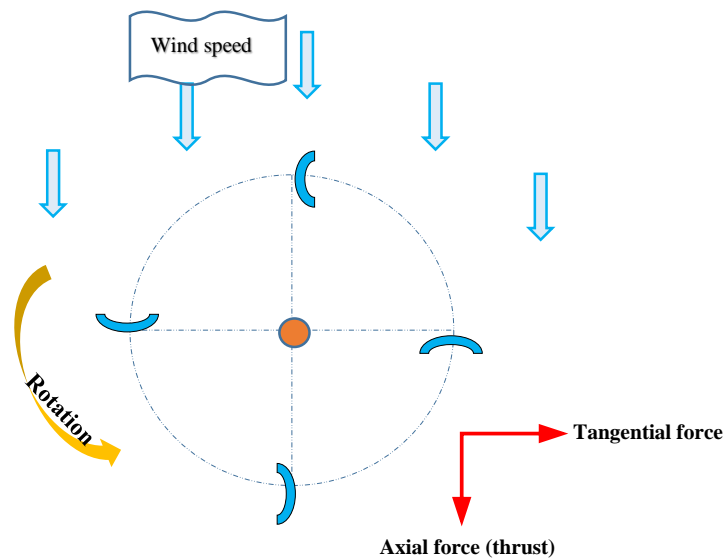


Figure 3.14: Different forces distribution and rotation of VAWT.

3.7 Experimental studies:

- **H form VAWT:**

H form was the first shape we tested it under different number blades and wind speeds:



Figure 3.15: Sixteen perpendicular to each other.



Figure 3.16: Ten blades perpendicular to each other.

Figures (3.15 and 3.16) shows the two from five shapes we created and tested in different wind speed, where the blades set perpendicular to each other and to the axis divided into 360° into the bases.

There are some tests results shown in the following table:

V (m/s)	N (rpm)	ω (rad/s)	λ (rad)	Δp (pas)	Pa (watt)	Vt (m/s)	Pt (watt)	Cp
2,9	21,7	2,272	0,235	1	5,378	0,682	0,245	0,046
4,2	36,7	3,843	0,275	3	16,336	1,153	1,245	0,076
5,2	64	6,702	0,387	7	31,004	2,011	5,067	0,163
6,3	85,19	8,921	0,425	10	55,135	2,676	9,635	0,175
8,4	101,93	10,674	0,381	13	130,691	3,202	14,986	0,115
10	118,18	12,376	0,371	16	220,500	3,713	21,385	0,097
12	140,38	14,701	0,368	21	381,024	4,410	33,341	0,088
12,6	147,54	15,450	0,368	24	441,083	4,635	40,047	0,091
14,2	187,75	19,661	0,415	30	631,355	5,898	63,702	0,101
		λ moy =	0,358				Cp moy =	0,106

Table 3.1: Characteristics of ten blades perpendicular to each other.

Note :

when we have reached 194,75 Rpm , the axis is broken due to the loosening of the lock nut because of axis material fragility (zinc).So we change the axis into a solid material.

- **V form VAWT:**

V form was the second shape we tested it under different number blades and wind speeds, Blades located in the lower base are 10.5 cm in from the locale position.



Figure 3.17: V form sixteen blades.



Figure 3.18: V form ten blades

V (m/s)	N (rpm)	ω (rad/s)	λ (rad)	Δp (pas)	Pa (watt)	Vt (m/s)	Pt (watt)	Cp
2,9	41,52	4,348	0,450	1	5,378	1,304	0,470	0,087
4,2	60,52	6,338	0,453	5	16,336	1,901	3,422	0,209
5,2	92,08	9,643	0,556	10	31,004	2,893	10,414	0,336
6,3	115,05	12,048	0,574	15	55,135	3,614	19,518	0,354
8,4	140,63	14,727	0,526	22	130,691	4,418	34,991	0,268
10	160,2	16,776	0,503	34	220,500	5,033	61,602	0,279
12	196,48	20,575	0,514	43	381,024	6,173	95,552	0,251
12,6	215,05	22,520	0,536	52	441,083	6,756	126,472	0,287
14,2	239,74	25,106	0,530	65	631,355	7,532	176,241	0,279
		λ moy =	0,516			Cp moy =		0,261

Table 3.2: Characteristics of ten blades V form.

- **A form VAWT:**

A form was the third shape we tested it under different number blades and wind speeds, Blades located in the upper base are 9.5 cm in from the locale position and left reverse the lower base beside.

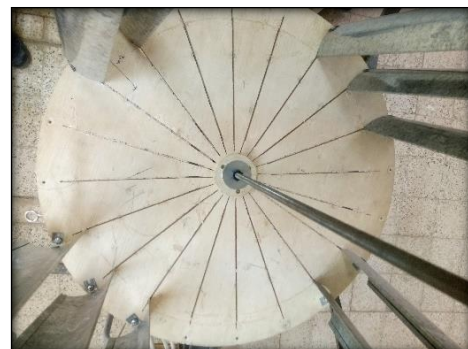


Figure 3.19: A form sixteen blades.

Figure 3.20: A form ten blades

V (m/s)	N (rpm)	ω (rad/s)	λ (rad)	Δp (pas)	Pa (watt)	Vt (m/s)	Pt (watt)	Cp
2,9	0	0,000	0,000	0	5,378	0,000	0,000	0,000
4,2	68,67	7,191	0,514	3	16,336	2,157	2,330	0,143
5,2	89,11	9,332	0,538	6	31,004	2,799	6,047	0,195
6,3	120,55	12,624	0,601	9	55,135	3,787	12,270	0,223
8,4	141,5	14,818	0,529	13	130,691	4,445	20,804	0,159
10	164,74	17,252	0,518	16	220,500	5,175	29,811	0,135
12	188,78	19,769	0,494	25	381,024	5,931	53,376	0,140
12,6	208,49	21,833	0,520	33	441,083	6,550	77,813	0,176
14,2	240,24	25,158	0,532	42	631,355	7,547	114,116	0,181
		λ moy =	0,472			C_p moy =		0,150

Table 3.3: Characteristics of ten blades A form.

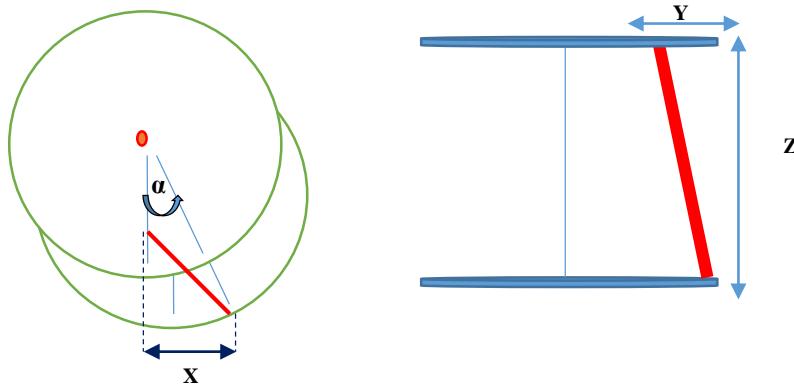


Figure 3.21: A form distance and inclination blades.

X	left reverse the lower base beside	5.7 cm
Y	distance from the locale position	9.5 cm
Z	Hight of turbine	60 cm
α	Degree between blades	18 °

Table 3.4: distance and inclination of A form blades.

- **H 3 form VAWT:**

H 3 forms was the fourth shape we tested with fifteen blades dispatched three by three blades all over the bases turbine under different wind speeds.



Figure 3.22: Fifteen blades perpendicular to each other three by three.

V (m/s)	N (rpm)	ω (rad/s)	λ (rad)	Δp (pas)	Pa (watt)	Vt (m/s)	Pt (watt)	Cp
2,9	31,89	3,340	0,345	3	5,378	1,002	1,082	0,201
4,2	53,34	5,586	0,399	8	16,336	1,676	4,826	0,295
5,2	76,57	8,018	0,463	12	31,004	2,406	10,392	0,335
6,3	100,45	10,519	0,501	20	55,135	3,156	22,721	0,412
8,4	118,07	12,364	0,442	26	130,691	3,709	34,719	0,266
10	131,06	13,725	0,412	35	220,500	4,117	51,879	0,235
12	159,38	16,690	0,417	45	381,024	5,007	81,115	0,213
12,6	168,81	17,678	0,421	58	441,083	5,303	110,733	0,251
14,2	183,5	19,216	0,406	74	631,355	5,765	153,575	0,243
		λ moy =	0,423				Cp moy =	0,272

Table 3.5: Characteristics of Fifteen blades perpendicular to each other three by three.

- **H 2 form VAWT:**

H 2 form was the fifth shape we tested with twenty blades dispatched two by two blades all over the bases turbine under different wind speeds.

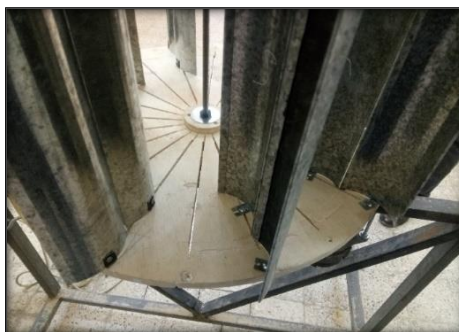


Figure 3.23: Twenty blades perpendicular to each other two by two.

V (m/s)	N (rpm)	ω (rad/s)	λ (rad)	Δp (pas)	Pa (watt)	Vt (m/s)	Pt (watt)	Cp
2,9	47,6	4,985	0,516	2	5,378	1,495	1,077	0,200
4,2	74,06	7,756	0,554	5	16,336	2,327	4,188	0,256
5,2	101,13	10,590	0,611	8	31,004	3,177	9,150	0,295
6,3	129,29	13,539	0,645	14	55,135	4,062	20,471	0,371
8,4	155	16,232	0,580	22	130,691	4,869	38,566	0,295
10	181,29	18,985	0,570	27	220,500	5,695	55,359	0,251
12	206,41	21,615	0,540	42	381,024	6,485	98,047	0,257
12,6	227,24	23,797	0,567	52	441,083	7,139	133,641	0,303
14,2	260,41	27,270	0,576	65	631,355	8,181	191,436	0,303
		λ moy =	0,573				Cp moy =	0,281

Table 3.6: Characteristics of twenty blades perpendicular to each other two by two.

- **S form VAWT:**

S form was the sixth shape we tested with twenty blades, Ten blades placed 10.5 cm in from local position and in opposite direction under different wind speeds.



Figure 3.24: S form blades shape.

V (m/s)	N (rpm)	ω (rad/s)	λ (rad)	Δp (pas)	Pa (watt)	Vt (m/s)	Pt (watt)	Cp
2,9	0	0	0		0	0,000	0	0
4,2	74,69	7,822	0,559	7	16,336	2,346	5,913	0,362
5,2	102,48	10,732	0,619	12	31,004	3,220	13,908	0,449
6,3	122,71	12,850	0,612	18	55,135	3,855	24,981	0,453
8,4	146,24	15,314	0,547	24	130,691	4,594	39,694	0,304
10	174,32	18,255	0,548	34	220,500	5,476	67,031	0,304
12	182,88	19,151	0,479	44	381,024	5,745	91,006	0,239
12,6	214,72	22,485	0,535	54	441,083	6,746	131,135	0,297
14,2	232,77	24,376	0,515	69	631,355	7,313	181,647	0,288
		λ moy =	0,490				Cp moy =	0,337

Table 3.7: Characteristics of S form blades.

- **One in One out form VAWT:**

One in One out form was the seventh shape we tested with twenty blades, Ten blades placed 10.5 cm in from local position and in same direction under different wind speeds.



Figure 3.25: One in One out blades form.

V (m/s)	N (rpm)	ω (rad/s)	λ (rad)	Δp (pas)	Pa (watt)	Vt (m/s)	Pt (watt)	Cp
2,9	38,97	4,081	0,422	3	5,378	0,122	0,132	0,025
4,2	58,29	6,104	0,436	6	16,336	1,831	3,955	0,242
5,2	78,49	8,219	0,474	10	31,004	2,466	8,877	0,286
6,3	104,85	10,980	0,523	16	55,135	3,294	18,973	0,344
8,4	130,31	13,646	0,487	24	130,691	4,094	35,371	0,271
10	153,71	16,096	0,483	31	220,500	4,829	53,891	0,244
12	176,89	18,524	0,463	40	381,024	5,557	80,023	0,210
12,6	204,63	21,429	0,510	54	441,083	6,429	124,973	0,283
14,2	223,86	23,443	0,495	66	631,355	7,033	167,099	0,265
		λ moy =	0,477				Cp moy =	0,241

Table 3.8: Characteristics of One in One out blades form.

Conclusion:

Different shapes type VAWT are designed and tested. All of them are fabricated and experimentally investigated in front of a subsonic wind tunnel. All these experiments tested at different wind speeds. Number of rotation and Power coefficients are determined from both the methods and compared.

The experimental setup has some issues, which could contribute some error during data acquisition.

CHAPTER

4

CHAPTER 4

Introduction:

To validate the cascade models for VAWT, Seven shapes were experimented, and their results compared to see their effects.

According to previous results in chapter three, we convert and try to combined between theme and we obtained a graphics curves.

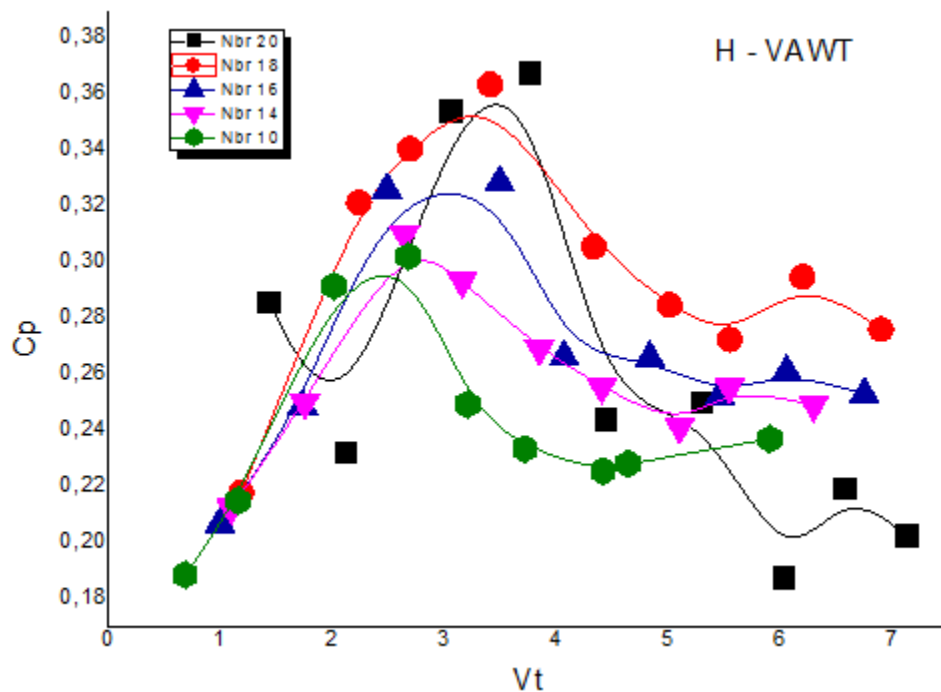
4.1 H form VAWT:

Figure 4.1: power coefficient and turbine speed of all blade H form shape.

(Figure 4.1) shows that power coefficient and turbine speed of twenty-blade shape in H form has the best results.

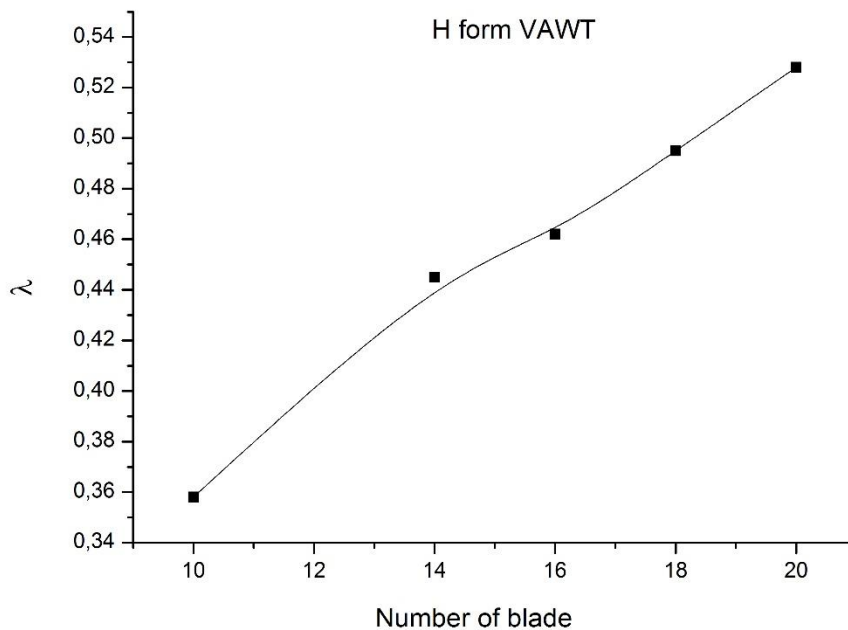


Figure 4.2: TSR and number of blade of all blade H form shape.

(Figure 4.2) described TSR and number of blad results of all blade shapes H form That shows increasing as the number of blades increases. Twenty blade shape has the highest result.

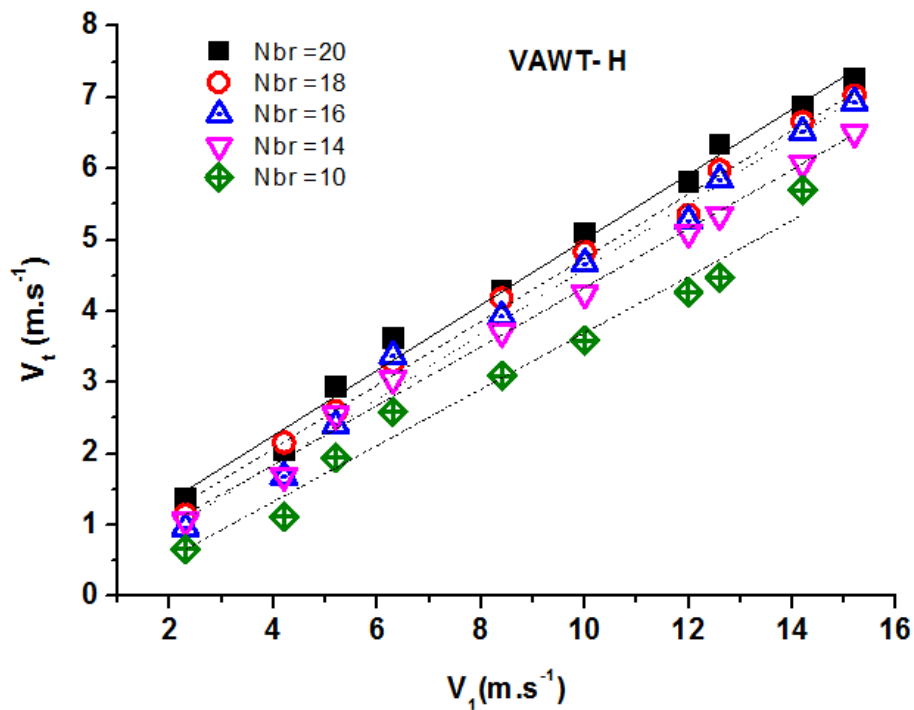


Figure 4.3: Speed turbine and wind speed of all blade H form shape.

(Figure 4.3) shows the curve between Speed turbine and wind speed of all blade shapes H form and what we see that there is a direct relationship, when wind speed rises so the turbine speed to. We observe that twenty blades shape has the best results.

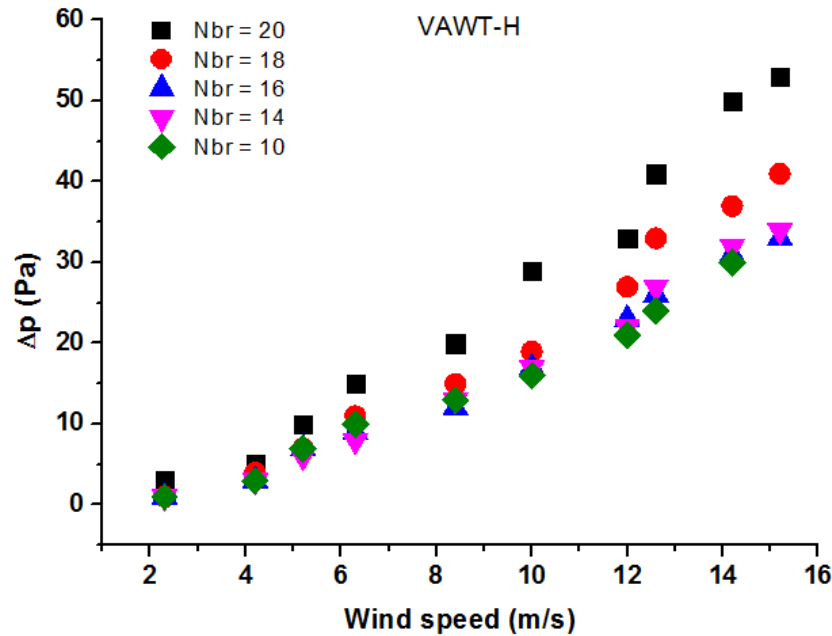


Figure 4.4: pressure differential and wind speed of all blade H form shape.

(Figure 4.4) shows the curve between pressure differential and wind speed of all blade shapes H form and what we see that there is a relation between them, when wind speed rises so the pressure differential to. We observe that twenty blades shape record the best result.

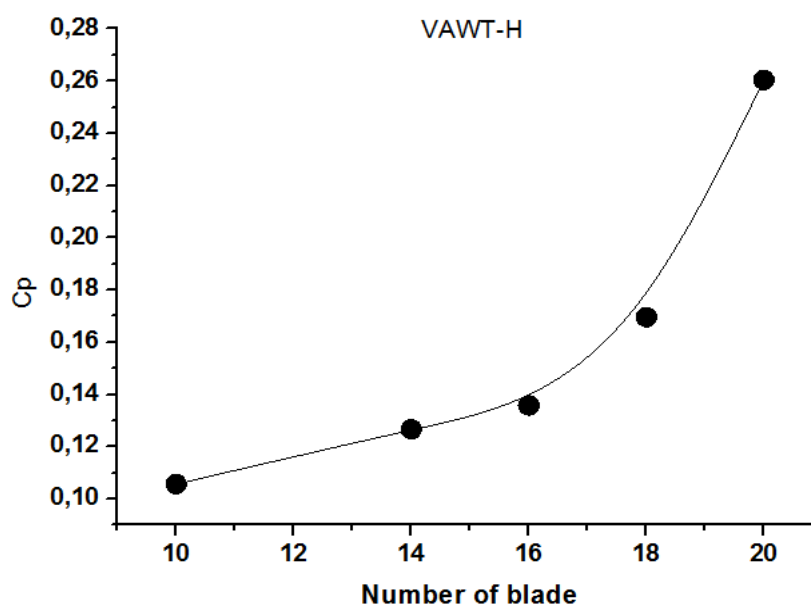


Figure 4.5: power coefficient and Number of blade of all blades H form shape.

(Figure 4.5) curve shows that in H form there is direct relationship between power coefficient and Number of blades

4.2 V form VAWT:

According to this results, we convert and try to combined between theme and we obtained a graphics curves.

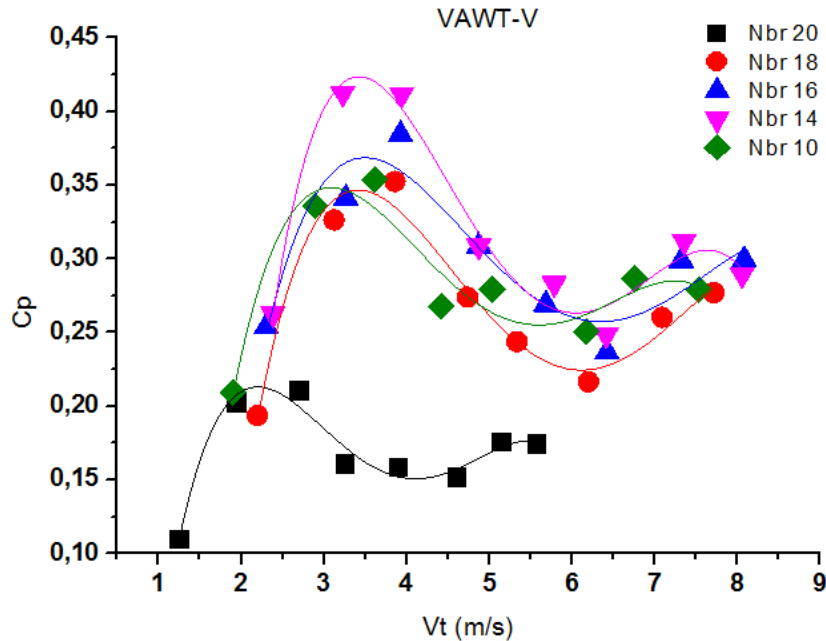


Figure 4.6: power coefficient and turbine speed of all blades V form shape.

(Figure 4.6) shows that power coefficient and turbine speed of all blade shapes V form, what we observe an important result in fourteen blades shape between [3-4](m/s) speed, unlike twenty blades shape which has the lowest results according to weight in first cause

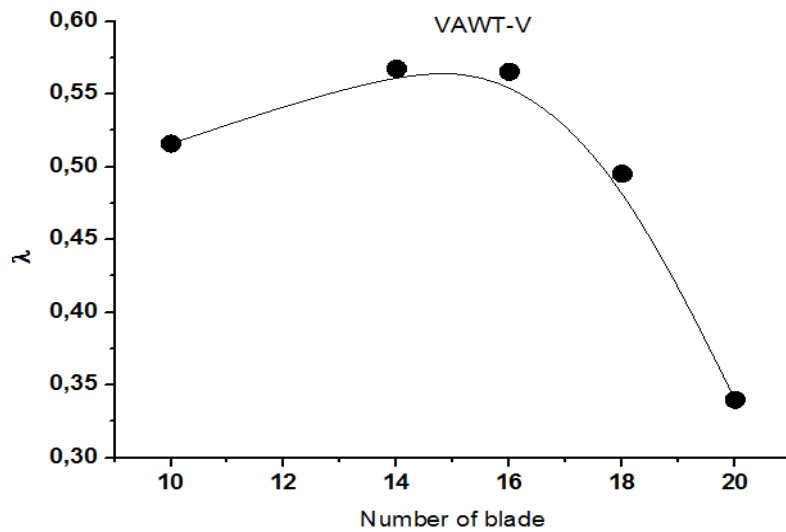


Figure 4.7: TSR and Number of all blades V form shape.

(Figure 4.7) curve shows TSR and Number of blades in V form. We observe the highest value TSR in fourteen and sixteen blades shape unlike twenty blade shape have the lowest value because of weight as the effective factor.

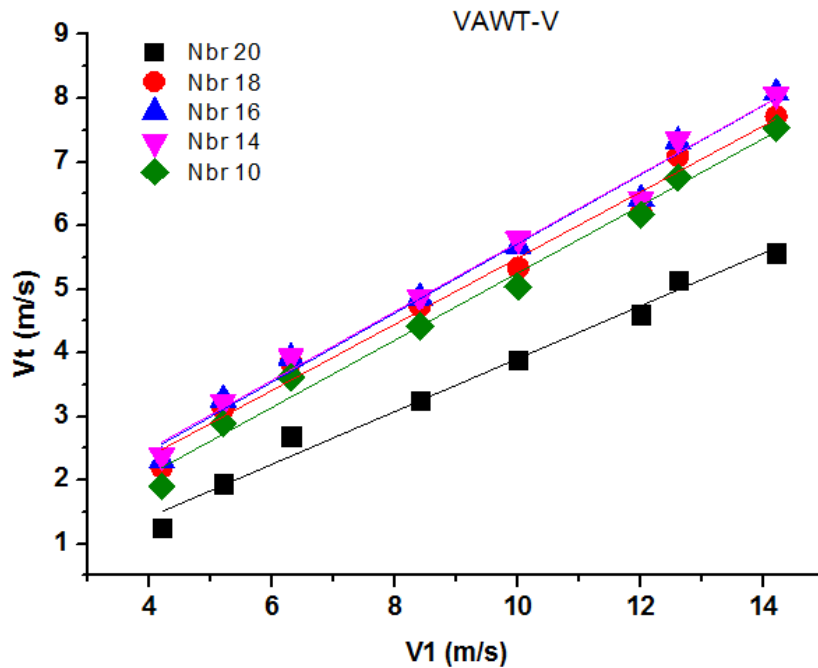


Figure 4.8: Speed turbine and wind speed of all blade V form shape.

(Figure 4.8) shows the curve between Speed turbine and wind speed of all blade shapes V form and what we see that there is a direct relationship, when wind speed rises so the turbine speed to. We observe that twenty blades shape has the lowest results.

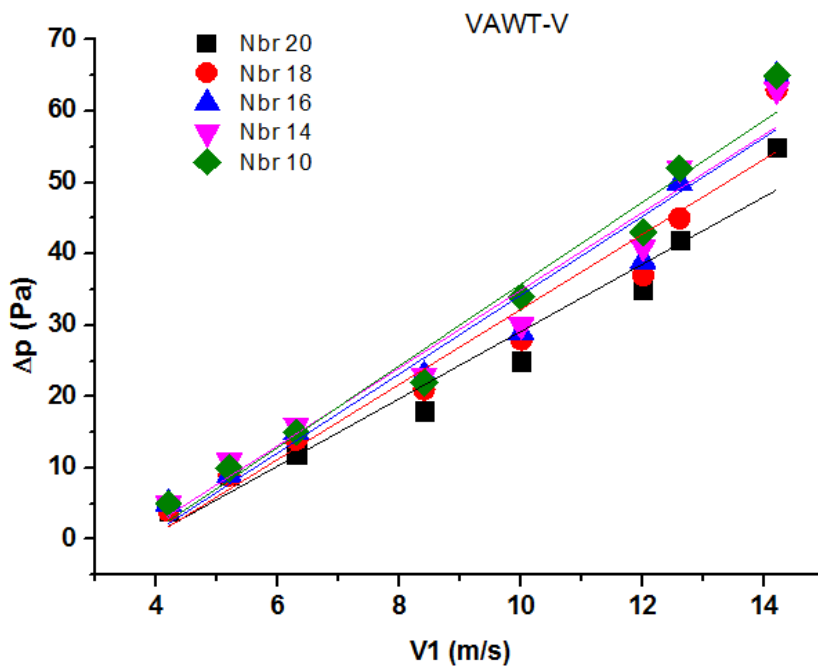


Figure 4.9: pressure differential and wind speed of all blade V form shape.

(Figure 4.9) shows the curve between pressure differential and wind speed of all blade shapes V form and what we see that there is a relation between them, when wind speed rises so the pressure differential to. We observe that ten blades shape record the best result.in the first speed twenty and eighteen blade shapes the rotor doesn't rotate and this according to the weight and the torque.

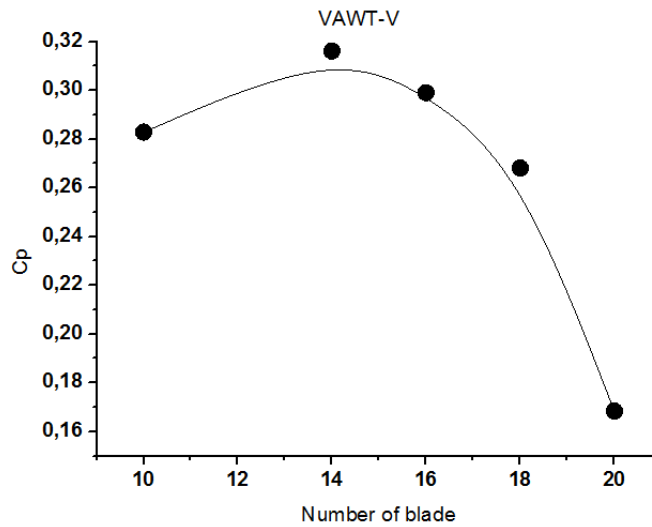


Figure 4.10: power coefficient and Number of blade of all blades V form shape.

(Figure 4.10) curve shows that in V form there is an inverse relationship between power coefficient and Number of blades. Fourteen blades shape record the highest result unlike twenty blade shape.

4.3 A form VAWT :

According to results, we convert and try to combine between them then obtained a graphics curves.

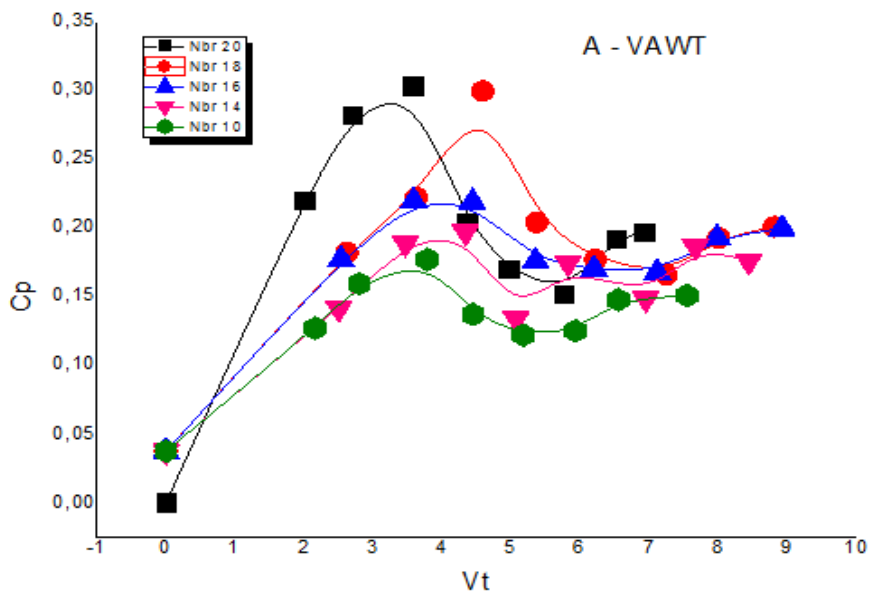


Figure 4.11: power coefficient and turbine speed of all blade shapes A form.

(Figure 4.11) shows that power coefficient and turbine speed of all blade shapes in A form, what we observe that ten and eighteen blades shape has the highly result between [3-5] (m/s).

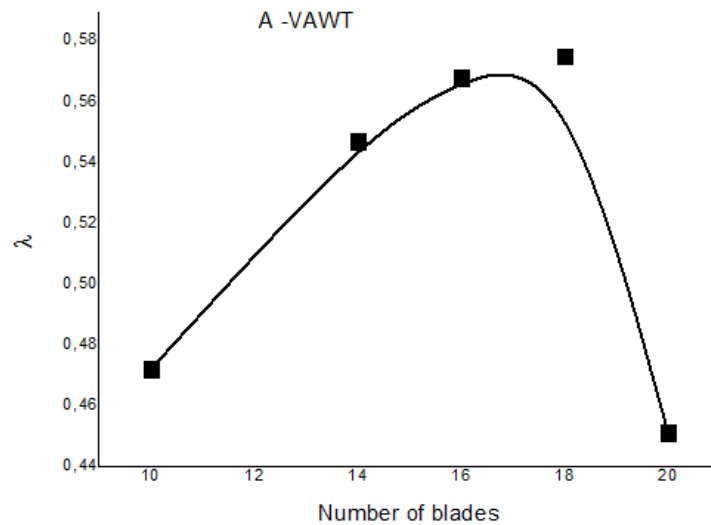


Figure 4.12: TSR and number of blade of all blade A form shape.

(Figure 4.12) described TSR and number of blade results of all blade shapes A form, we observe that TSR rises until his best result in eighteen blades shape then a free fall.

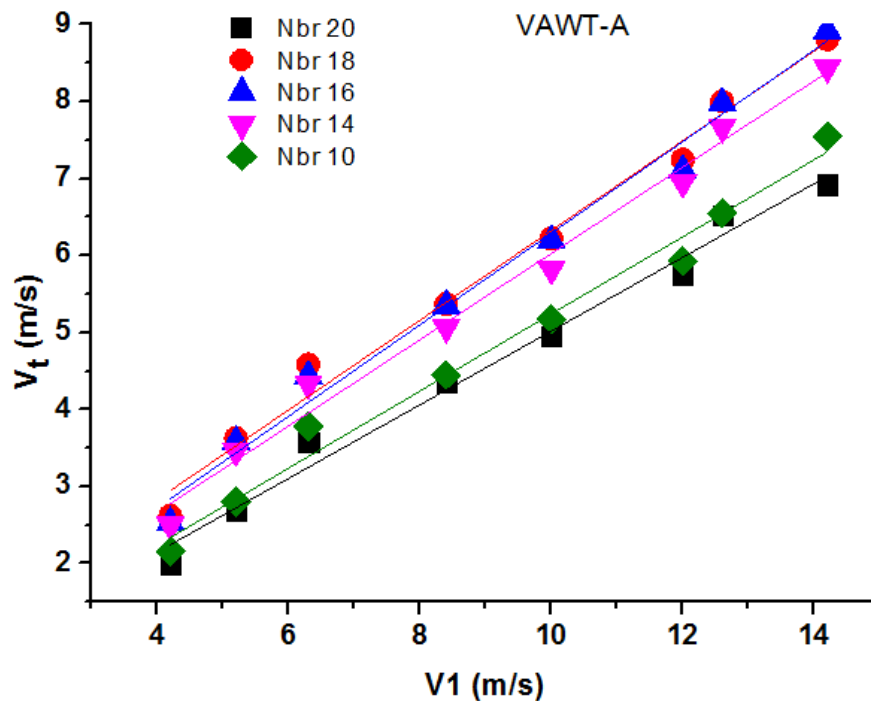


Figure 4.13: Speed turbine and wind speed of all blade A form shape.

(Figure 4.13) shows the curve between Speed turbine and wind speed of all blade shapes A form and what we see that there is a direct relationship, when wind speed rises so the

turbine speed to.

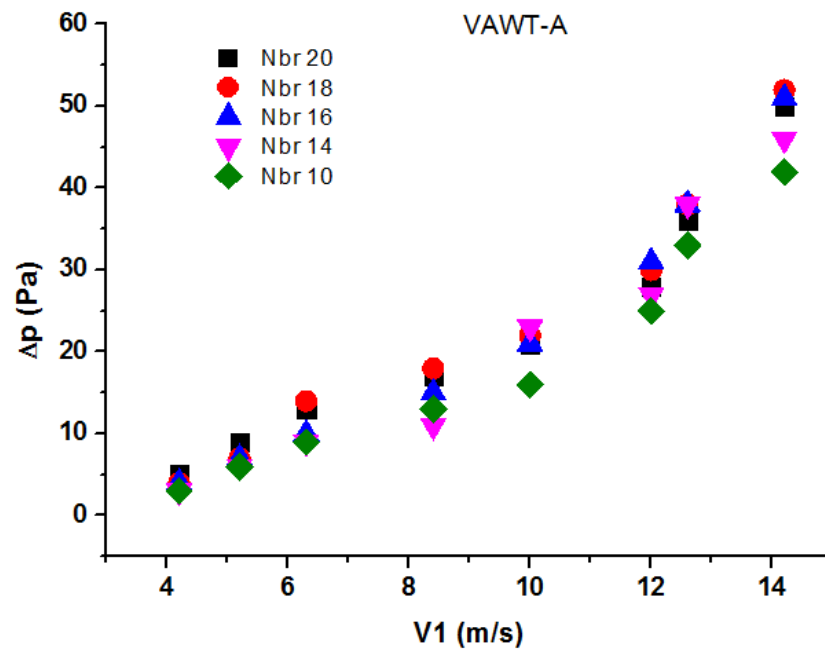


Figure 4.14: pressure differential and wind speed of all blade A form shape.

(Figure 4.14) shows the curve between pressure differential and wind speed of all blade shapes A form, when wind speed rises so the pressure differential to. We observe that results are quietly close.

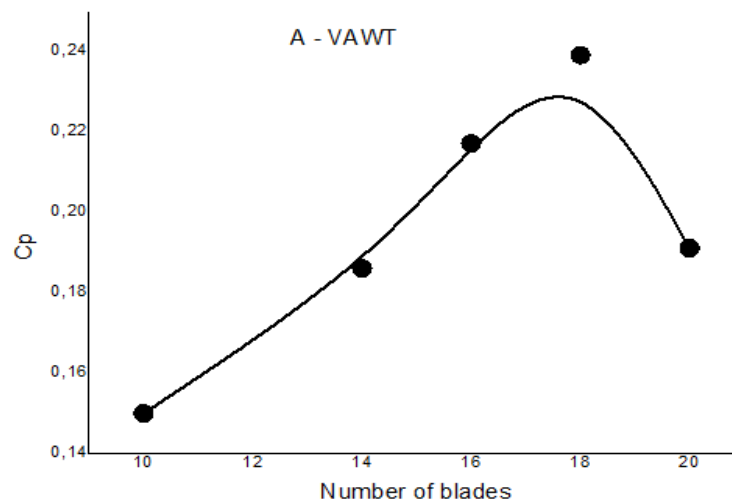


Figure 4.15: power coefficient and Number of blades of A form shape.

(Figure 4.15) curve shows relationship between power coefficient and Number of blades in A form. We noticed an upsurge of results until the highest value of power coefficient in eighteen blade shape then a fall in twenty blade shape.

4.4 H 3 form VAWT:

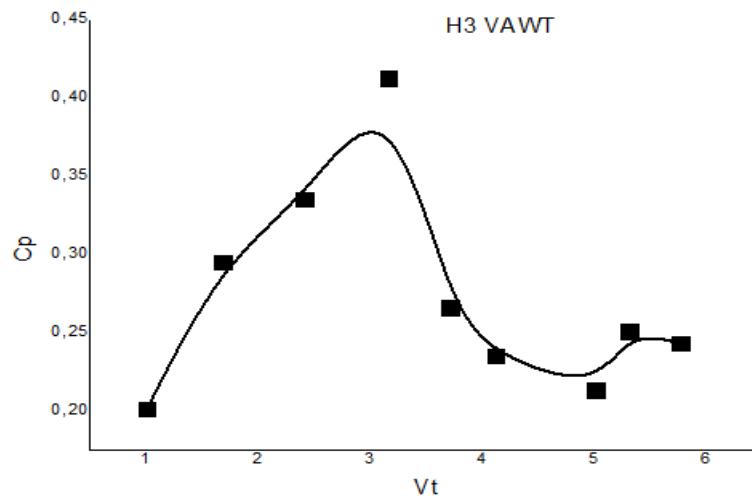


Figure 4.16: Power coefficient and wind speed of H 3 form.

(Figure 4.16) described Power coefficient and wind speed results of H 3 shapes form, there is an important difference unlike the previous H form shapes .

4.5 H 2 form VAWT:

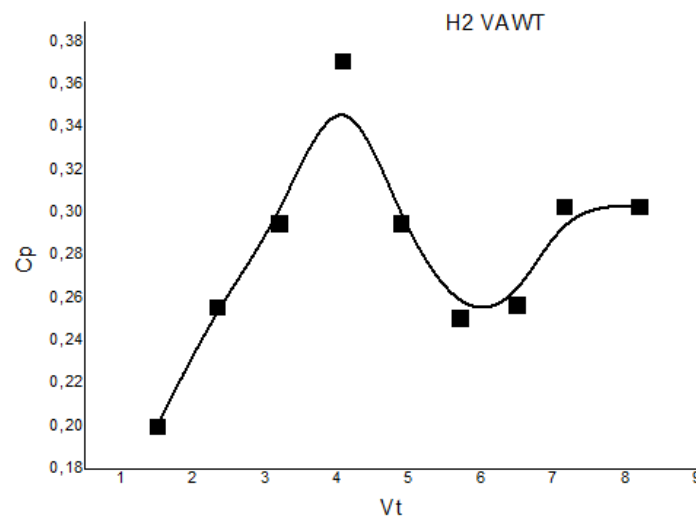


Figure 4.17: Power coefficient and wind speed of H 2 form.

(Figure 4.17) described Power coefficient and wind speed results of H 2 shapes form, we observe an improvement when $Vt = 4$ m/s.

4.6 S form VAWT:

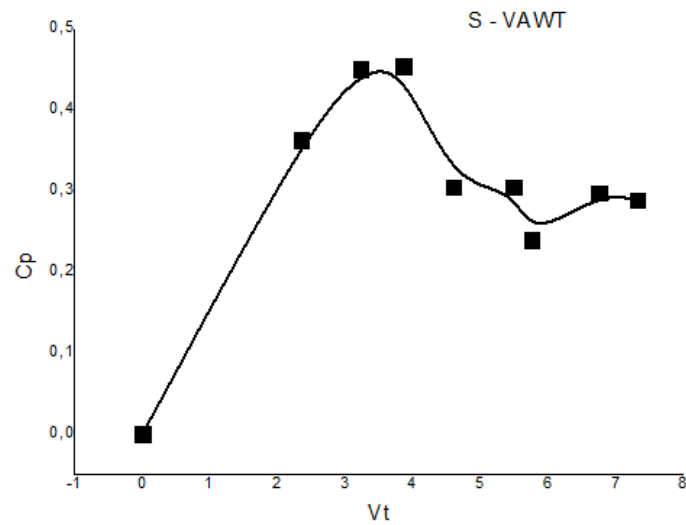


Figure 4.18: Power coefficient and wind speed of S form.

(Figure 4.18) described Power coefficient and wind speed results of S shapes form, we record the highest result between [3-4](m/s), then a fluctuation from 4.5 (m/s) results.

4.7 One in One out form VAWT:

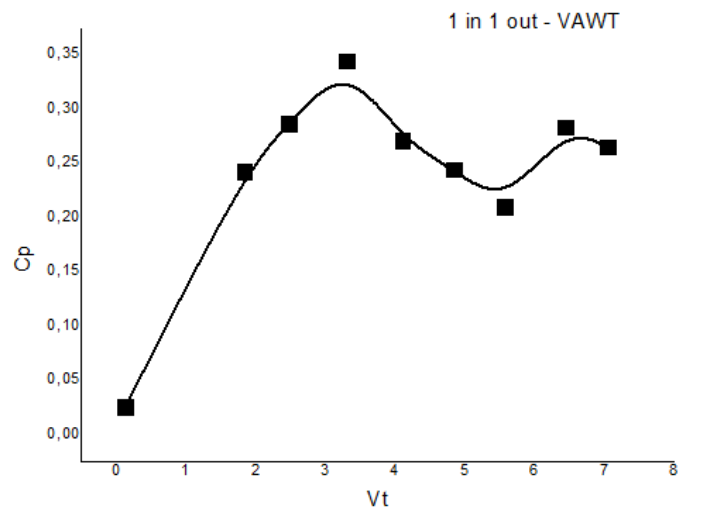


Figure 4.19: Power coefficient and wind speed of One in One out form.

(Figure 4.19) described Power coefficient and wind speed results of S form shape.

Conclusion:

According to the experience results we observe about:

- H , V and A shapes that when wind speed equal to 5.2 m/s and 6.3 m/s we registered the best power coefficient result (C_p) unlike other wind speed values.
- H3 , H2 , S and 1in1out shapes that when wind speed equal to 4.2m/s and 5.2m/s we registered the best power coefficient(C_p) unlike other wind speed values.

We record the highest values of power coefficient for all shapes :

Shape	Turbine speed (V_t) m/s	Power coefficient (C_p)watt	Blades number
H	6.3	0.367	20
V	5.2	0.413	14
A	6.3	0.419	18
H3	6.3	0.412	15
H2	6.3	0.371	20
S	6.3	0.453	20
1in1out	6.3	0.344	20

Table 4.1: highest values of power coefficient for all shapes.

CONCLUSION

The main purpose of this work is to enhance the performance VAWT which includes efficiency and range of operation. An experimental study for different blades shapes was carried out. It has been investigated to obtain different values of $TSR(\lambda)$, power coefficient(C_p) and turbine speed ratio(V_t) using measurement instruments and mathematical formulations. Furthermore, seven rotors performance has been compared and identified between their results to validate the best model. Power coefficient (C_p) obtained as a function of the turbine speed in order to determine the best sectional airfoil that can be used in Darrius turbine.

It hoped that in future this type of turbines are economically viable and competitive opposite to other types of energy transformation, because of its easy maintenance and installation.

In the future it will be made more experiments to validate other shapes of VAWT. There is some proposed designs to work on.

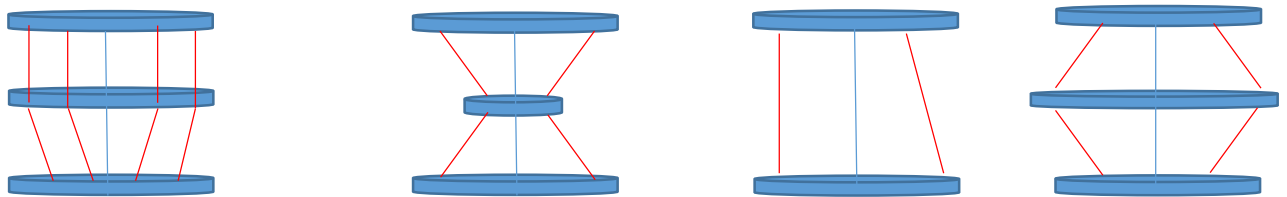


Figure 4.20: designs for future experience.

REFERENCE

- [1] [HTTPS://WWW.IEA.ORG/DATA-AND-STATISTICS/CHARTS/ELECTRICITY-GENERATION-AND-POWER-SECTOR-CO2-EMISSIONS-IN-ADVANCED-ECONOMIES-1971-2019](https://www.iea.org/data-and-statistics/charts/electricity-generation-and-power-sector-co2-emissions-in-advanced-economies-1971-2019). (ACCESS ON 02/05/2020-18:14)
- [2] [HTTPS://WWW.GE.COM/RENEWABLEENERGY/WIND-ENERGY/WHAT-IS-WIND-ENERGY](https://www.ge.com/renewableenergy/wind-energy/what-is-wind-energy)). (ACCESS ON 02/05/2020-18:36)
- [3] Z. WANG, M. ZHUANG LEADING-EDGE SERRATIONS FOR PERFORMANCE IMPROVEMENT ON A VERTICAL-AXIS WIND TURBINE AT LOW TIP-SPEED-RATIOS APPL ENERGY, 208 (2017).
- [4] E. HAU, WIND-TURBINES FUNDAMENTALS, TECHNOLOGIES, APPLICATION, ECONOMICS, SPRINGER, 2000.
- [5] [HTTPS://WWW.RESEARCHGATE.NET/FIGURE/THE-MAJOR-WIND-TURBINE-TYPES-INCLUDING-THE-PROPELLER-TYPE-HORIZONTAL-AXIS-WIND-TURBINE_FIG3_263161316](https://www.researchgate.net/figure/The-major-wind-turbine-types-including-the-propeller-type-horizontal-axis-wind-turbine_fig3_263161316)(ACCESS ON 07/05/2020-13:20)
- [6] MOHAMMAD M. BASHAR COMPUTATIONAL AND EXPERIMENTAL STUDY ON VERTICAL AXIS WIND TURBINE IN SEARCH FOR AN EFFICIENT DESIGN.
- [7] [HTTP://WWW.SOLAR.EXCLUSS.COM/WIND-POWER/HOW-MAGLEVS-WORK.HTML](http://www.solar.exclus.com/wind-power/how-maglevs-work.html).(ACCESS ON 09/05/2020-09:45)
- [8] [HTTPS://WWW.RESEARCHGATE.NET/FIGURE/DIFFERENT-TYPES-OF-DARRIEUS-ROTOR-VAWT_FIG1_313893605](https://www.researchgate.net/figure/Different-types-of-darrieus-rotor-VAWT_fig1_313893605). (ACCESS ON 09/05/2020-10:22)
- [9] [HTTPS://WWW.RESEARCHGATE.NET/FIGURE/FIG-4-GENERAL-VIEW-OF-TYPE-A-HYBRID-ROTOR-CONFIGURATION_FIG1_271656129](https://www.researchgate.net/figure/Fig-4-general-view-of-type-a-hybrid-rotor-configuration_fig1_271656129). (ACCESS ON 09/05/2020-10:52)
- [10] [HTTP://LARGE.STANFORD.EDU/COURSES/2011/PH240/JAFFER2/](http://large.stanford.edu/courses/2011/ph240/jaffer2/).(ACCESS ON 11/05/2020-11:10)
- [11] [HTTPS://WWW.IEA.ORG/FUELS-AND-TECHNOLOGIES/WIND](https://www.iea.org/fuels-and-technologies/wind).(ACCESS ON 11/05/2020-11:41)
- [12] [HTTPS://LIBRARY.WWINDEA.ORG/GLOBAL-STATISTICS/](https://library.wwindea.org/global-statistics/). ACCESS ON 15/05/2020-08:10)
- [13] GWEC / GLOBAL WIND REPORT 2018 APRIL 2019.
- [14] S. K. DHIMAN (AUTHOR), 2018, EFFECT OF SOME DESIGN PARAMETERS: A PERFORMANCE TEST ON VAWT.
- [15] WIND ENERGY EXPLAINED: THEORY, DESIGN AND APPLICATION, SECOND EDITION JAMES MANWELL, JON MCGOWAN, AND ANTHONY ROGERS 2009 JOHN WILEY & SONS, LTD
- [16] COOPER, P. & KENNEDY, O. C. (2004). DEVELOPMENT AND ANALYSIS OF A NOVEL VERTICAL AXIS WIND TURBINE.
- [17] TEST OF IMPELLER TYPE VAWT IN WIND TUNNEL (A. Y. QASIM, R. USUBAMATOV AND Z.M. ZAIN) SCHOOL OF MANUFACTURING ENGINEERING, UNIVERSITY MALAYSIA PERLIS, ULU PAUH, ARAU, 02600 PERLIS, MALAYSIA..
- [18] ANALYSIS AND IMPLEMENTATION OF A DRAG-TYPE VERTICAL-AXIS WIND TURBINE FOR SMALL

[19] PERFORMANCE AND DYNAMIC CHARACTERISTICS OF A MULTI STAGES VERTICAL AXIS WIND TURBINE. EL ARABI ATTIA, HESHAM SABER, HASSAN EL GAMAL . © JVE INTERNATIONAL LTD. JOURNAL OF VIBROENGINEERING. SEP 2016, VOL. 18, ISSUE 6. ISSN 1392-8716

[20] EXPERIMENTAL VALIDATION OF THE POWER ENHANCEMENT OF A PAIR OF VERTICAL-AXIS WIND TURBINES ANTOINE VERGAERDE A , TIM DE TROYER A , * , LIEVEN STANDAERT A , JOANNA KLUCZEWSKA-BORDIER B , DENIS PITANCE B , ALEXANDRE IMMAS B , C , FRED ERIC SILVERT B , MARK C. RUNACRES A A VRIJE UNIVERSITEIT BRUSSEL, PLEINLAAN 2, 1050, BRUSSELS, BELGIUM B NENUPHAR, 1, RUE DU PROFESSEUR CALMETTE, 59000, LILLE, FRANCE C UNIVERSITY OF CALIFORNIA, BERKELEY, 6141 ETCHEVERRY HALL, BERKELEY, CA, 94720-1740, USA.

[21] OPTIMAL BLADE PITCH FUNCTION AND CONTROL DEVICE FOR HIGH-SOLIDITY STRAIGHT BLADED VERTICAL AXIS WIND TURBINES YOU-LIN XU , YI-XIN PENG, SHENG ZHAN DEPARTMENT OF CIVIL AND ENVIRONMENTAL ENGINEERING, THE HONG KONG POLYTECHNIC UNIVERSITY, HONG KONG

[22] T. MICHA PREM KUMAR, S. SERALATHAN, R. GOPALAKRISHNAN, T. MOHAN AND V. HARIRAM, EXPERIMENTAL DATA OF THE STUDY ON H- ROTOR WITH SEMI-ELLIPTIC SHAPED BLADED VERTICAL AXIS WIND TURBINE, DATA IN BRIEF, [HTTPS://DOI.ORG/10.1016/J.DIB.2018.06.063](https://doi.org/10.1016/j.dib.2018.06.063)

[23] REAL-TIME MAXIMIZED POWER GENERATION OF VERTICAL AXIS WIND TURBINES BASED ON CHARACTERISTIC CURVES OF POWER COEFFICIENTS VIA FUZZY PULSE WIDTH MODULATION LOAD REGULATION PONGPAK LAP-ARPARAT, THANANCHAI LEEPHAKPREEDA. /SCHOOL OF MANUFACTURING SYSTEMS AND MECHANICAL ENGINEERING, SIRINDHORN INTERNATIONAL INSTITUTE OF TECHNOLOGY, THAMMASAT UNIVERSITY, P.O. BOX 22, THAMMASAT-RANGSIT POST OFFICE, PATHUM THANI, 12121, THAILAND.

[24] ARIAN HOSSEINIA, NAVID GOUDARZIB, DESIGN AND CFD STUDY OF A HYBRID VERTICAL-AXIS WIND TURBINE BY EMPLOYING A COMBINED BACH-TYPE AND H-DARRIEUS ROTOR SYSTEMS.